ISTANBUL TECHNICAL UNIVERSITY ★ GRADUATE SCHOOL OF SCIENCE ENGINEERING AND TECHNOLOGY

PRODUCTION OF 3D SCAFFOLDS FROM NATURAL POLYMERS AND THEIR CHARACTERISATION

MSc THESIS

Burak AĞBABA

Department of Molecular Biology-Genetics and Biotechnology

Molecular Biology-Genetics and Biotechnology Programme

JUNE 2016

ISTANBUL TECHNICAL UNIVERSITY ★ GRADUATE SCHOOL OF SCIENCE ENGINEERING AND TECHNOLOGY

PRODUCTION OF 3D SCAFFOLDS FROM NATURAL POLYMERS AND THEIR CHARACTERISATION

MSc THESIS

Burak AĞBABA
(521131124)

Department of Molecular Biology-Genetics and Biotechnology

Molecular Biology-Genetics and Biotechnology Programme

Thesis Advisor: Assoc. Prof. Dr. Fatma Neşe KÖK

JUNE 2016

Burak Ağbaba, a MSc student of ITU Graduate School of Science, Engineering and Technology student ID 521131124, successfully defended the thesis entitled "PRODUCTION OF 3D SCAFFOLDS FROM NATURAL POLYMERS AND THEIR CHARACTERISATION", which he prepared after fulfilling the requirements specified in the associated legislations, before the jury whose signatures are below.

Thesis Advisor :	**Assoc Prof Dr Fatma Neşe KÖK** Istanbul Technical University	.....
Jury Members :	**Prof Dr Ayten YAZGAN KARATAŞ** Istanbul Technical University	…….....
	Prof Dr Sedef TUNCA GEDİK Gebze Technical University	.....

Date of Submission : 02 May 2016
Date of Defense : 08 June 2016

To my family,

FOREWORD

Firstly, I would like to express my sincere gratitude to my supervisor Assoc. Prof. Dr. Fatma Neşe KÖK for her guidance, support, patience, understanding and encouragement during my masters programme.

I would also like to thank Assist Prof Dr Sakip Önder and Dr Barbaros Akkurt for their time and effort for scanning electron microscope images and fourier transform infrared spectra of scaffolds and Prof Dr Ahmet Gül for allowing us to use FTIR spectroscopy in his laboratory.

Additionally, I want to verbalise my special thanks to my lab-mate İnasÖzcan for her great help, support, assistance and contribution to my masters programme beginning from the first day to the end even in relatively busy, tiring and exhausting times, and to Ayşe BuseÖzdabak and BerenŞen, my lab-mates with whom I worked in the same laboratory sharing ideas, helping and supporting each other. Working together with such a good team means a lot to me on my way to success and happy end.

Before and during my masters programme, I had the opportunity to work with great people. A huge bunch of thanks goes to my current and former colleagues and managers for their understanding, support and encouraging during that stressful and tiring masters programme period.

I would also like to acknowledge the financial support of Istanbul Technical University through Graduate Thesis Funding Project (grant no: 39484).

Above all, I would like to thank Gülsemin Ağbaba, my mother, Nuri Ağbaba, my father, and LütfiyeAğbaba, my sister, and really appreciate for their endless and invaluable faith in me, for being always by my side, supporting my ideas, actions and activities for my future plans, for encouraging me to pursue and realise my dreams.

May 2016 Burak AĞBABA

TABLE OF CONTENTS

Page

FOREWORD ..... **ix**
TABLE OF CONTENTS ..... **xi**
ABBREVIATIONS ..... **xiii**
SYMBOLS ..... **xv**
LIST OF TABLES ..... **xvii**
LIST OF FIGURES ..... **xix**
SUMMARY ..... **xxi**
ÖZET ..... **xxiii**
1. INTRODUCTION **1**
1.1 Purpose of Thesis **1**
1.2 Tissue Engineering **2**
1.3 Scaffolds **3**
1.4 Scaffold Fabrication Techniques **4**
1.4.1 Freeze-drying **4**
1.4.2 Solvent casting and particulate leaching **7**
1.4.3 Gas foaming **7**
1.4.4 Electro-spinning **8**
1.5 Use of Synthetic and Natural Polymers in Tissue Engineering **9**
1.5.1 Synthetic polymers **10**
1.5.1.1 Non-biodegradable synthetic polymers **10**
1.5.1.2 Biodegradable synthetic polymers **10**
1.5.2 Natural polymers **11**
1.5.2.1 Proteins **11**
1.5.2.2 Polysaccharides **16**
1.6 Non-polymeric Materials **18**
1.6.1 Ceramics **18**
1.6.2 Bioactive glass **18**
1.7 Bone Tissue Regeneration **19**
1.7.1 Bone tissue structure **19**
1.7.2 Bone tissue regeneration approaches **20**
1.7.3 Bone tissue engineering **21**
2. MATERIALS AND METHODS **23**
2.1 Materials **23**
2.1.1 Chemicals **23**
2.1.2 Solutions **23**
2.1.3 Laboratory equipment **23**
2.2 Methods **23**
2.2.1 Fibroin extraction from *Bombyx mori* silkworm cocoons **23**
2.2.2 Preparation of silk fibroin-gelatin blend solutions **25**
2.2.3 Lyophilisation of silk fibroin-gelatin blend solutions **26**

2.2.4 Characterisation of silk fibroin-gelatin composite scaffolds..... **26**
2.2.4.1 Analysis with scanning electron microscopy…..**26**
2.2.4.2 Analysis with fourier transform infrared spectroscopy…….**26**
2.2.5 Water-uptake test of silk fibroin-gelatin composite scaffolds **26**
2.2.6 3-day biodegradation test of silk fibroin-gelatin composite scaffolds **27**
2.2.7 Biodegradation test of silk fibroin-gelatin composite scaffolds..... **28**
2.2.8 Biomineralisation test of silk fibroin-gelatin composite scaffolds..... **28**
3. RESULTS AND DISCUSSION..... **31**
3.1 Characterisation of Scaffolds **31**
3.1.1 Morphology of scaffolds **31**
3.1.2 Effect of methanol treatment on chemical structures of scaffolds **35**
3.2 Water-uptake and 3-day in vitro Biodegradation Analysis of Scaffolds..... **40**
3.3 *in vitro* Biodegradation Analysis of Scaffolds **42**
3.3.1 Weight loss during the biodegradation analysis..... **42**
3.2.2 Morphology change during the biodegradation analysis **45**
3.4 *in vitro* Biomineralisation Analysis of Scaffolds **46**
3.4.1 Scanning electron microscopy analysis..... **46**
3.4.2 Fourier transform infrared spectroscopy analysis **53**
4. CONCLUSIONS AND RECOMMENDATIONS **61**
REFERENCES **63**
APPENDICES **71**
APPENDIX A **73**
APPENDIX B **75**
APPENDIX C **77**
APPENDIX D **79**
CURRICULUM VITAE **81**

ABBREVIATIONS

2D	**:** Two-dimensional
3D	**:** Three-dimensional
BMP	**:** Bone Morphogenic Protein
CO_3^{2-}	**:** Carbonate
CO_3	**:** Carbon Trioxide
CS	**:** Chondroitin Sulfate
ECM	**:** Extra Cellular Matrix
et. al.	**:** *et aliae*
FDA	**:** Food and Drug Administration
FTIR	**:** Fourier Transform Infrared Spectroscopy
GAG	**:** Glycosaminoglycan
Gly	**:** Glycine
HA	**:** Hyaluronic Acid
HEPES	**:** 4-(2-hydroxyethyl)-1-piperazineethanesulfonic acid
HPO_4^{2-}	**:** Monohydrogen Phosphate
LiBr	**:** Lithium Bromide
LVD	: Leucine-Asparagine-Valine
mSBF	**:** Modified Simulated Body Fluid
OH^-	**:** Hydroxyl
PBS	**:** Phosphate Buffered Saline
PCL	**:** Poly (caprolactone)
PDS	**:** Poly (dioxanone)
PEG	**:** Poly (ethylene glycol)
PG	**:** Proteoglycan
PGA	**:** Poly (glycolide)
PLA	**:** Poly (lactide)
PO_4^{3-}	**:** Phosphate
PTMC	**:** Poly (trimethylene carbonate)
RGD	**:** Arginine-Glycine-Aspartic Acid
SEM	**:** Scanning Electron Microscopy
ssCO_2	**:** Supercritical Saturated Carbon Dioxide
US	**:** United States

SYMBOLS

%	**:** Per cent
%T	**:** % Transmittance
atm	**:** Atmosphere
cm^{-1}	**:** Wavenumber
g	**:** Gram
kDa	**:** Kilodalton
M	**:** Molar
mg	**:** Milligram
mL	**:** Mililitre
mmHg	**:** Millimetres of Mercury
pH	**:** Power of Hydrogen
psi	**:** Pounds per Square Inch
rpm	**:** Revolutions per Minute
U/mL	**:** Units per Volume Solution Concentration
v/v %	**:** Volume/Volume per cent
w/v %	**:** Weight/Volume per cent
^{o}C	**:** Degree Centigrade

LIST OF TABLES

Page

Table 1.1 : Basic characteristics of scaffolds for tissue engineering applications. **..... 5**
Table 1.2 : Biodegradable natural polymers and their properties. **..... 15**
Table 1.3 : Biodegradable and widely used natural polysaccharides and their properties. **..... 18**
Table 2.1 : Compositions of silk fibroin-gelatin blend solutions.. **..... 26**
Table 3.1 : Results of water-uptake and 3-day *in vitro* biodegradation tests.. **..... 40**
Table 3.2 : Results of *in vitro* biodegradation tests for a) F3-G1 samples and b) F2-G2 samples. **..... 43**
Table 3.3 : FTIR absorption bands of synthesised hydroxyapatite chemical groups **53**

LIST OF FIGURES

Page

Figure 1.1 : An overview of tissue engineering approach **3**
Figure 1.2 : Phase diagram showing the triple point of water at 0.01 ^{o}C and 0.00603 atm. **7**
Figure 1.3 : General description for gas foaming method. **8**
Figure 1.4 : General scheme for electro-spinning method. **9**
Figure 1.5 : Examples for some commercially available collagen scaffolds. **12**
Figure 1.6 : The hydrophobic β-sheet structure of silk fibroin embedded in the amorphous regions, which are hydrophilic and hold moisture (water molecules are shown by blue dots). **14**
Figure 1.7 : The structure of natural bone tissue showing structural and cellular components. **20**
Figure 3.1 : SEM images of F4-G0 (a), F3-G1 (b), F2-G2 (c), F1-G3 (d) and F0-G4 (e) samples. **32**
Figure 3.1 (continued) : SEM images of F4-G0 (a), F3-G1 (b), F2-G2 (c), F1-G3 (d) and F0-G4 (e) samples. **33**
Figure 3.1 (continued) : SEM images of F4-G0 (a), F3-G1 (b), F2-G2 (c), F1-G3 (d) and F0-G4 (e) samples. **34**
Figure 3.2 : Comperative FTIR spectra of F3-G1 samples: The black line indicates the sample with methanol treatment, whereas the red line indicated the sample without methanol treatment. **37**
Figure 3.3 : Comperative FTIR spectra of F2-G2 samples: The black line indicates the sample with methanol treatment, whereas the red line indicated the sample without methanol treatment. **38**
Figure 3.4 : Comperative FTIR spectra of F1-G3 samples: The black line indicates the sample with methanol treatment, whereas the red line indicated the sample without methanol treatment. **39**
Figure 3.5 : Comparative biodegradation results of F3-G1 and F2-G2 samples.. ..... **44**
Figure 3.6 : SEM images of F3-G1 samples after the 1st (a), 2nd (b), 3rd (c) and 4th week of *in vitro* biodegradation test... ..... **45**
Figure 3.7 : SEM images of F2-G2 samples after the 1st (a), 2nd (b), 3rd (c) and 4th week of *in vitro* biodegradation test... ..... **46**
Figure 3.8 : SEM images of F3-G1 samples after the 1st (a), 4th (b) and 7th (c) days of *in vitro* biomineralisation test with 1x mSBF. **47**
Figure 3.8 (continued): SEM images of F3-G1 samples after the 1st (a), 4th (b) and 7th (c) days of *in vitro* biomineralisation test with 1x mSBF. **48**
Figure 3.9 : SEM images of F3-G1 samples after the 1st (a), 4th (b) and 7th (c) days of *in vitro* biomineralisation test with 3x mSBF. **48**
Figure 3.9 (continued): SEM images of F3-G1 samples after the 1st (a), 4th (b) and 7th (c) days of *in vitro* biomineralisation test with 3x mSBF. **49**

Figure 3.10 : SEM images of F2-G2 samples after the 1st (a), 4th (b) and 7th (c) days of *in vitro* biomineralisation test with 1x mSBF. **50**
Figure 3.10 (continued) : SEM images of F2-G2 samples after the 1st (a), 4th (b) and 7th (c) days of *in vitro* biomineralisation test with 1x mSBF. **51**
Figure 3.11 : SEM images of F2-G2 samples after the 1st (a), 4th (b) and 7th (c) days of *in vitro* biomineralisation test with 3x mSBF. **52**
Figure 3.11 (continued): SEM images of F2-G2 samples after the 1st (a), 4th (b) and 7th (c) days of *in vitro* biomineralisation test with 3x mSBF. **53**
Figure 3.12 : Comparative FTIR spectra of F3-G1 samples without (b) and after the 1st (c), 4th (d) and 7th (a) days in biomineralisation test with 1x mSBF. **55**
Figure 3.13 : Comparative FTIR spectra of F3-G1 samples without (b) and after the 1st (c), 4th (d) and 7th (a) days in biomineralisation test with 3x mSBF.... **56**
Figure 3.14 : Comparative FTIR spectra of F2-G2 samples without (b) and after the 1st (c), 4th (d) and 7th (a) days in biomineralisation test with 1x mSBF.... **59**
Figure 3.15 : Comparative FTIR spectra of F2-G2 samples without (b) and after the 1st (c), 4th (d) and 7th (a) days in biomineralisation test with 3x mSBF.... **59**

PRODUCTION OF 3D SCAFFOLDS FROM NATURAL POLYMERS AND THEIR CHARACTERISATION

SUMMARY

Composite 3D scaffolds with different blending ratios of silk fibroin and gelatin as natural polymers were produced by freeze-drying method within the scope of this study. The total polymer ratio of the scaffolds was 4% (w/v) and they were named based on their polymer contents as follows: 4% (w/v) silk fibroin, 3% (w/v) silk fibroin-1% (w/v) gelatin, 2% (w/v) silk fibroin-2% (w/v) gelatin, 1% (w/v) silk fibroin-3% (w/v) gelatin and 4% (w/v) gelatin being F4-G0, F3-G1, F2-G2, F1-G3 and F4-G0, respectively. According to the SEM images of these samples, F3-G1, F2-G2 and F1-G3 composite scaffolds had homogeneous porous structures and therefore selected for water-uptake and 3-day *in vitro* biodegradation test that was studied with three different enzyme concentrations (0.05, 0.1 and 0.2 U/mL). They were also treated with methanol and their FTIR spectra showed that this treatment led to β-sheet formation in F3-G1 and F2-G2 samples.

Once the three scaffold groups were immersed in PBS solution, the F2-G2 samples exhibited the highest water-uptake capacity (1271%), which was 797% and 1053% for F3-G1 and F1-G3 samples, respectively. The F1-G3 samples, which comprised the highest gelatin content, had the highest degradation rate at all enzyme concentrations tested for the 3-day biodegradation assay, whereas the F3-G1 samples had the lowest degradation ratio in all cases. The F2-G2 samples showed similar behaviour with F3-G1 sample except the one with the highest enzyme concentration in which an accelerated degradation was observed. As a result, the F3-G1 and F2-G2 samples and the enzyme concentration of 0.05 U/mL were selected for the main 28-day biodegradation test.

The average remaining weight ratio of the F3-G1 and F2-G2 samples was 50% and 42%, respectively, at the end of the 28-day biodegradation test. The degradation rate of the F3-G1 samples was lower than that of the F2-G2 samples during the first 7 days of the test. At the end of the 2nd week, the average remaining weight percentage was almost the same for all samples. Additionally, the SEM images of almost all degraded samples showed more porous structures indicating bulk erosion.

In order to induce hydroxyapatite formation on the surfaces of the samples, the F3-G1 and the F2-G2 scaffolds were immersed in either 1x or 3x mSBF for different time intervals of 1, 4 and 7 days. The SEM images of the F3-G1 samples showed no hydroxyapatite formation, except the one treated with 1x mSBF and collected after the 1st day. For F2-G2 samples, only the SEM images of the ones treated with 1x or 3x mSBF and collected after the 4th day did not exhibit any hydroxyapatite crystals. On the other hand, some absorption peaks that are characteristic to the some chemical groups of hydroxyapatite crystals were detected in the FTIR spectra of the all F3-G1 and F2-G2 samples that may be formed due the hydroxyapatite formation on the surfaces of the scaffolds.

DOĞAL POLİMERLER İLE HAZIRLANAN DOKU İSKELELERİNİN YAPIMI VE KARAKTERİZASYONU

ÖZET

Yaralanmalar, kazalar ve hastalıklar nedeniyle organ veya dokularda meydana gelen hasarlar veya işlevsel yetmezlikler dünya genelinde birçok insan için büyük bir sorun teşkil etmektedir. Bu noktada, doku mühendisliği, biyoloji, kimya ve mühendislik ilkelerinden faydalanarak özellikle kemik, kıkırdak, karaciğer ve deri dokularında meydana gelen hasarların iyileştirilmesi amacıyla mevcut geleneksel tedavi yöntemlerine ek olarak yeni tedavi fırsatları sunmaktadır. Transplantasyon için uygun otolog ve allojenik dokuların eksikliği ve sentetik dokuların biyouyumluluğunun düşük olması yerleşik tedavi seçenekleri arasında görülen başlıca sorunlardan olup hastalıkların hızlı progresyonu, uygun bağışçıların bulunamaması ve pahalı medikal uygulamalar da bu tedavilerin dezavantajları arasında gösterilmektedir. Bu gibi nedenlerden ötürü kısmen veya tamamen kaybedilmiş veya zarar görmüş organ veya dokuların işlevsel olanlar ile değiştirilmesi için yeni teknolojiler geliştirilmesi modern rejeneratif tıbbın odak noktaları arasında yer almaktadır.

Yeni yapay dokuların oluşturulması amacıyla doku mühendisliği, farklı özellikteki biyomalzemeleri kullanarak doku iskelesi (“scaffold”) adı verilen, yeni dokuların oluşması ve gelişmesi için uygun bir mikroçevre ve histolojik organizasyon sağlayan üç boyutlu yapıların üretilmesini sağlamaktadır. Hücre bağlanması, çoğalması, farklılaşması ve üç boyutlu doku oluşumu için uygun yüzey kimyasına ve yapısına sahip olması gereken doku iskeleleri için seçilen biyomalzemelerin hedef doku özelliklerine özgü bir şekilde seçilmesi ve kullanılması doku mühendisliği uygulamalarının başarısı için büyük önem taşımaktadır. Ayrıca, büyüme faktörleri gibi biyolojik moleküllerin doku iskelelerine katılması ile doku iskelelerinin hücre aktivitelerini istenildiği şekilde yönlendirme yeteneği de iyileştirilebilmektedir. Doku mühendisliğinin üç temel unsuru olan doku iskelesi, biyolojik moleküller ve hücreler, uygulamalardan elde edilen sonuçlar üzerinde büyük rol oynamaktadır. Bu üç unsur arasında ise doku iskeleleri, yeni doku oluşumun her bir aşamasında başından sonuna dek yer aldığından ayrıca dikkati çekmektedir.

Biyomalzeme olarak adlandırılan; sentetik polimer, metal, alaşım veya seramik formunda laboratuvarda üretilen sentetik malzemelerin veya doğal polimerlerin kullanılması ile üretilen doku iskeleleri, sundukları yapısal, mekanik ve biyolojik özelllikler nedeniyle doku mühendisliği uygulamaları için her geçen gün daha fazla önem kazanmaktadır. Hücrelerin metabolik işlevleri için gerekli besin maddelerinin sağlanması ve metabolik aktiviteler sonucu ortaya çıkan atıkların uzaklaştırılması için uygun mikroçevreyi sağlaması gereken doku iskelelerinin birbiri ile bağlantılı ve toplam yüzey alanını artıran gözenekelere sahip olması; doğal dokununkine yüksek oranda benzeyen ekstraselüler matriks oluşumu, hücre bağlanması, çoğalması ve farklılaşması için uygun altyapıyı sunması; yeni doku oluşumuna dek doku işlevsel ve mekanik özelliklerini koruması gerekmektedir.

Polimer, metal ve seramik gibi malzemeler doku iskelelerinin üretilmesi amacıyla yaygın olarak kullanılmaktadır. Birçok klinik araştırmanın odak noktası olan sentetik ve doğal polimerlerin kendi içlerinde sunduğu farklı avantajlar ve dezavantajlar bulunmaktadır. Sentetik polimerler kolayca işlenebilip değiştirilebilirken doğal polimerler yüksek biyouyumluluk sağlamaktadır. Öte yandan, farklı doku tipleri farklı fiziksel, mekanik ve degradasyon özellikleri gerektirdiğinden tüm doku tiplerine yönelik olarak kullanılabilecek tek bir biyomalzeme tipi bulunmamaktadır.
Doku iskelelerinin üretiminde kullanılan doğal polimerlerden olan ipek fibroini, yüksek oksijen geçirgenliği, biyouyumluluğu, kontrol edilebilir biyodegradasyonu ve mekanik özellikleri nedeniyle yapay kan damarları, ameliyat iplikleri gibi biyomedikal amaçlı uygulamalarda kullanım için FDA tarafından onaylanmış bir biyomalzeme olup doku mühendisliği uygulamaları çerçevesinde fibroblastlar, osteoblastlar ve hepatositler için uygun bir yapısal destek malzemesidir.
Bir başka doğal polimer olan jelatin, kollajenin hidrolize edilmesi ile elde edilmektedir. Biyouyumluluğu, biyodegradasyon özelliği ve düşük maliyeti nedeniyle ilaç, medikal ve gıda sanayilerinde sıkça kullanılmakta olan jelatin düşük mekanik dayanıklılığı sebebiyle doku mühendisliği uygulamaları için farklı malzemeler ile kombinasyon halinde uygulanmaktadır.
Hedef doku tipi ve özelliklerine bağlı olarak istenilen yapısal, kimyasal ve biyolojik özelliklere sahip doku iskelelerinin üretilmesi için farklı yöntemlerden yararlanılmaktadır. Dondurarak kurutma, tuz giderme, gaz köpürtme ve elektroçekme yöntemleri doku mühendisliği uygulamaları kapsamında yaygın olarak kullanılan yöntemlerdir.
Liyofilizasyon olarak da adlandırılan dondurarak kurutma yöntemi süblimleşme temeline dayanan iki aşamalı bir kurutma işlemi olup doku iskelesi üretimi için hazırlanmış örnekten dondurulmuş çözücünün, çoğunlukla suyun, uzaklaştırılmasını sağlamaktadır. Bir malzemenin dondurularak kurutulması için önce dondurulması ardından da dondurulmuş sıvının yüksek vakumlu ortamda süblimleşmesi ve böylelikle yalnızca kurumuş bileşenleri geride bırakması gerekmektedir. Kurumakta olan yüz ile yoğunlaştırıcı arasında proses sırasında oluşan konsantrasyon gradiyenti liyofilizasyondaki sıvının uzaklaştırılması için itici güç görevi görmektedir. Sıvı kristalleri, örnek için hazırlanmış çözelti tamamen derişik duruma gelene dek çözeltiden ayrılmaya devam etmektedir. Doku iskeleleri için önemli parametreler olarak bilinen gözenek büyüklüğü ve gözenek alanı liyofilizasyon süresi ve sıcaklığı değiştirilerek ayarlanabilmektedir. Basit ve kolay olmasına karşın dondurarak kurutma yöntemi zaman ve enerji tüketimi açısından dezavantajlı da olabilmektedir.
Bu çalışma, kemik dokusunda meydana gelen hasarların onarılmasını ve kemik doku yenilenmesini sağlayan biyouyumlu, biyobozunur, doğal polimerik yapıya sahip ve doğal kemik yapısına benzeyen üç boyutlu doku iskelesi üretimini ve karakterizasyonunu amaçlamaktadır. Bu amaçla, ipek böceği kozalarından elde edilen ipek fibroini ile ticari olarak temin edilen jelatinin farklı oranlardaki kombinasyonu ile doku iskeleleri üretilmiş, üretilen bu iskeleler yapısal olarak incelenmiş ve su tutma, biyobozunma ve biyomineralizasyon testlerine tabi tutulmuştur.
İpek fibroin/jelatin oranları 100/0, 75/25, 50/50, 25/75 ve 0/100 olan ve sırasıyla F4-G0, F3-G1, F2-G2, F1-G3 ve F0-G4 olarak adlandırılan doku iskelelerinin morfolojileri Taramalı Elektron Mikroskobu (*Scanning Electron Microscopy, SEM*) ile incelenmiştir. Bu incelemere göre, kompozit örneklerdeki jelatin oranı arttıkça örneklerin yüzey yapılarının gözenekliliğinin arttığı ve örneklerin homojen gözenekli bir yapı sergiledikleri görülmüştür. F4-G0 örnekleri ayrı katmanlı yapılara sahipken

F0-G4 örnekleri ise homojen gözeneklilik açısından diğer örneklere üstünlük sağlamıştır. Kompozit örnekler arasında en iyi gözenekli yapıyı F1-G3 örnekleri göstermişken bu incelemelere dayanarak F3-G1, F2-G2 ve F1-G3 örnekleri, homojen gözenekli yapıları ve genel morfolojileri nedeniyle, metanolün örneklerin kimyasal yapısı üzerindeki etkiyi gözlemlemek amacıyla Fourier Transform Infrared (FTIR) Spektroskopisi ile incelenmiş ve ayrıca su tutma ve 3 günlük biyodegradasyon testlerine tabi tutulmuştur.

FTIR Spektroskopisi sonuçlarına göre örneklerin metanol ile muamele edilmesi F3-G1 ve F2-G2 örneklerinin ikincil yapılarında β tabakası oluşumundan kaynaklanabilecek kısmi değişikliğe neden olurken F1-G3 örneklerinde ise bir değişiklik görülmemiştir. Üç kompozit doku iskelesi arasında en yüksek su tutma oranı %1271 ile F2-G2 örneklerinde görülürken bu oran F3-G1 ve F1-G3 örnekleri için sırasıyla %797 ve %1053 olmuştur. Üç farklı enzim konsantrasyonu (0,05, 0,1 ve 0,2 U/mL) ile gerçekleştirilen üç günlük biyobozunma testleri, jelatin oranı ve enzim konstrasyonu arttıkça kompozit doku iskelelerinde görülen bozulma oranının da arttığını göstermiştir. 3 günlük deneyden elde edilen sonuçlar değerlendirildiğinde asıl biyobozunma çalışmasının 28 gün süreceği göz önüne alındığında, bu çalışma için F3-G1 ve F2-G2 örneklerinin seçilmesi ve enzim derişiminin 0,05 U/mL olması kararlaştırılmıştır.

F3-G1 ve F2-G2 örneklerinin 28 gün süren biyobozunma testi sonunda jelatin oranı yüksek olan F2-G2 örneklerinde %58 oranında bozulma görülürken bu oran F3-G1 örnekleri için %50 olarak kaydedilmiştir. Bununla birlikte, testin ilk 7 günü süresince F2-G2 örneklerinde F3-G1 örneklerine kıyasla daha hızlı bir bozunma gözlemlenmiş, 14 gün sonunda ise tüm örnekler için bozunma sonrası geriye kalan ortalama örnek ağırlığı oranı hemen hemen aynı olmuştur. Testin 7., 14., 21. ve 28. günleri sonunda alınan örneklerin morfolojileri ise genel olarak test öncesindeki morfolojilerinden farklılık göstermiş, örnek yapısı daha gözenekli bir hal almıştır.

F3-G1 ve F2-G2 örnekleri için ayrıca 7 gün süren bir biyomineralizasyon testi uygulanmıştır. Bu test ile örnekler 1x ve 3x olmak üzere iki farklı derişimdeki değiştirilmiş yapay vücut sıvısı (*modified simulated body fluid, mSBF*) ile muamele edilmiş ve kemik dokusunun önemli bir kısmını teşkil eden hidroksiapatit oluşumu testin 1., 4. ve 7. günü sonunda alınan örnekler için SEM ve FTIR Spekroskopisi ile incelenmiştir. SEM sonuçlarına göre, F3-G1 örneklerinin tümü için yalnızca 1x mSBF ile muamele edilen 1. gün örneklerinde hidroksiapatit oluştuğu görülmüş, F2-G2 örneklerinde ise her iki derişimdeki mSBF için 4. gün örnekleri hariç tüm örneklerde hidroksipatit oluşumu meydana gelmiştir. Biyomineralizasyon testinin daha iyi değerlendirilebilmesi için örneklerin FTIR spektrumlarının incelenmesiyle hidroksiapatit oluşumu için karakteristik kimyasal gruplara ait absorpsiyon bantları her iki mSBF derişiminde de F3-G1 ve F2-G2 örnekleri için görülmüş ve bu durum biyomineralizasyonun gerçekleşmesi olarak yorumlanmıştır.

1. INTRODUCTION

1.1 Purpose of Thesis

Tissue and organ defects or failures because of injuries, accidents or other damages are a major health problem for many people worldwide. At this point, tissue engineering emerges as an expanding field of applied biology and biomedical engineering making use of chemistry, biology and engineering principles in order to create new treatment opportunities to existing conventional interventions for damages of bone, cartilage, liver or skin tissues.

In order to produce new artificial tissues, tissue engineering uses biomaterials to construct three-dimensional templates, called scaffolds, which serve as an environment necessary for complete tissue formation and development. These scaffolds need to possess a surface chemistry and structure enabling cell attachment, proliferation, differentiation and 3D tissue formation. For this reason, designing appropriate biomaterials specific to properties of tissue of interest play an important role in the success of tissue engineering approaches. Additionally, biological molecules such as growth factors can be incorporated into scaffolds to improve the construct's capability to direct activities of seeded cells. Each of three major components of tissue engineering, scaffolds, bioactive molecules and cells, have significant effects on the outcomes of this field.

In the current study, a biocompatible and biodegradable 3D scaffold was fabricated using a blend of two different natural polymers, silk fibroin and bovine gelatin for bone tissue regeneration and repair. For this purpose, silk fibroin extracted from *Bombyxmori* silk worm cocoons and bovine gelatin purchased from a commercial supplier were used in different concentrations and the resultant scaffolds were subjected to water-uptake, biodegradation and biomineralisation tests in order to compare and evaluate the effect of blending ratios on the behaviour of scaffolds.

1.2 Tissue Engineering

Loss or failure of an organ and tissue as a result of an injury, disease or any kind of damage is a major health problem that many people are suffering from [1, 2]. Hurdles in early therapies centred on the lack of autologous and allogenic tissues suitable for transplantation and poor biocompatibility of synthetic tissue for grafting or transplantation [2]. Donor shortages, rapid progressions of diseases, expensive and inconvenient applications also limit conventional therapies [3]. For this reason, developing new technologies to replace or restore lost or damaged organs and tissues is a particular goal for modern regenerative medicine [4].

As an emerging science consisting of and applying mainly molecular biology and material engineering principles and methods, tissue engineering aims to develop biological substitutes for organs and tissues that have been damaged or lost their functions partially or completely [5, 6]. These biological substitutes must mimic histological organisation and function of organs and tissues they are established for [3]. To engineer new tissues, three major components are required: the right type of cells, a scaffold enabling attachment, proliferation and if needed differentiation of these cells, and signalling molecules such as growth factors for cell differentiation to desired cell lineage (Figure 1.1). Among these components, scaffolds play an important role in tissue engineering applications since they are involved in each and every step of new tissue formation [7, 8].

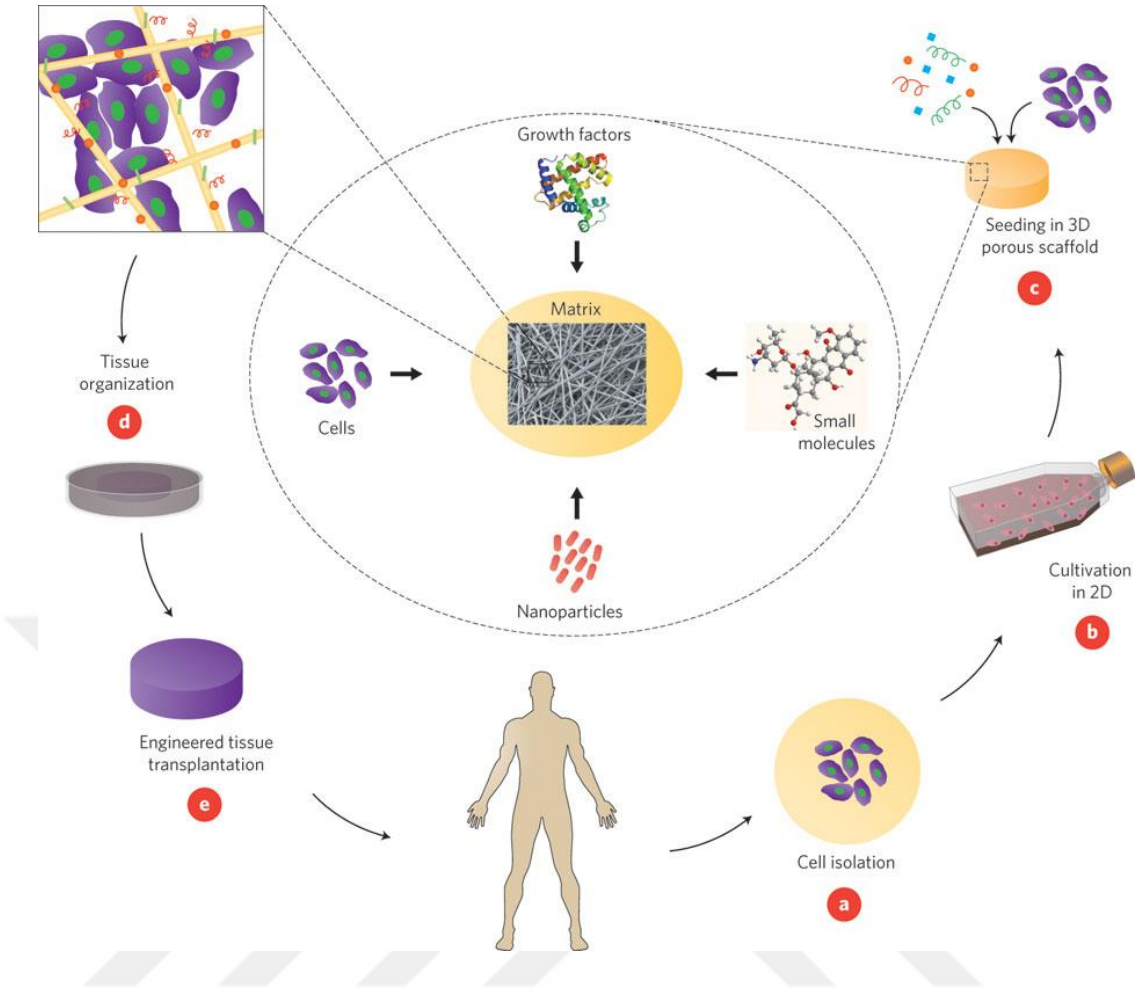

Figure 1.1: An overview of tissue engineering approach [9].

1.3 Scaffolds

Establishing a three-dimensional matrix for both *in vitro* and *in vivo* new tissue formation with desired structure and function is an important challenge in tissue engineering since it should be designed as an appropriate environment for supply of nutrients and removal of waste materials for seeded cells to survive [2].

Scaffolds, three-dimensional matrices fabricated from synthetic as well as natural polymers named biomaterials, have gained popularity and attraction due to structural, mechanical and biological properties they present for tissue engineering approaches [7, 10]. These scaffolds need to possess not only appropriate pore size, but also interconnected pores providing high surface area in order to provide a framework for cell adhesion, proliferation, differentiation and extracellular matrix formation highly similar to that of native tissue [7, 9-13]. Mechanical properties however should not deterioate with increasing porosity and should be able to sustain the tissue until the

new tissue formation. Some properties that are needed for a successful tissue engineering scaffold was given in Table 1.1.

When compared with those from synthetic polymers, scaffolds produced using natural polymers are providing non-toxicity, good cell attachment and reasonable biocompatibility for avoiding unwanted host responses with minimal immunogenicity [14, 15]. Both chemical and architectural properties of scaffolds have a particular impact on new tissue formation: an excellent surface chemistry enables cell attachment, proliferation and differentiation whereas adequate mechanical properties maintain structure and functions of scaffolds after implantation and during new tissue formation at implant site [15, 16]. Therefore, fabrication methods such as freeze-drying, salt-leaching, electro-spinning are under development in order to prepare suitable constructs for regeneration of various tissue types such as skin, cartilage, bone, nerve, and liver [1, 16].

1.4 Scaffold Fabrication Techniques

Several different methods have been developed and employed in order to manufacture scaffolds with desired structural, chemical and biological properties based on target tissue type using synthetic or natural materials [17]. Among these methods, freeze-drying, salt-leaching, gas foaming and electro-spinning are the ones that are widely used for tissue engineering applications.

1.4.1 Freeze-Drying

Freeze-drying, also called lyophilisation, is a two-step process of drying based on sublimation principle that removes frozen water from the sample prepared for scaffold fabrication [18, 19]. It is also one of the most studied scaffold preparation methods due to its simplicity and mild process conditions [13].

Table 1.1: Basic characteristics of scaffolds for tissue engineering applications [9].

Properties	Remarks
Bioresorbable	Foreign material and bulk degradation products should be eliminated from body by natural pathways
Controlled porosity with interconnected pores	Tailor-made cellular adhesion, growth, extracellular matrix secretion, angiogenesis, nutrition and oxygen transport without compromising mechanical strength
Biodegradable	Breakdown products of macromolecular degradation should not be toxic or immunogenic
Controlled pore structure	To provide greater diffusivity and higher diffusion coefficient for waste removal and nutrient transport
High surface area-to-volume ratio	For increased cell density, cell adhesion, proliferation, migration, and differentiation
Mechanical stability	Mechanical properties should match the replaced natural tissue to withstand *in vivo* stimuli
Three-dimensional templating	To assist cellular in-growth and provide a natural three-dimensional *in vivo* microenvironment
Mimic natural ECM	Properties and structures should be matched with natural ECM components to coordinate with biological cues
Cellular compatibility	Scaffold surfaces must show cellular compatibility and should not repel cells
Vascular support	To support angiogenesis and healthy regeneration
Biocompatible	Should not provoke any rejection, inflammation, immune response, etc.
Surface modifiable	Scaffold surfaces should allow chemical or biomolecularfunctionalisation to increase cell-material interactions
Non-toxic	Should not evoke toxicity to tissues
Non-immunogenic	Immunogenic response to tissue must not be evoked
Non-corrosive	Should not become corroded at physiological pH and body temperature
Sterilisable	Surfaces must be receptive to sterilization processes to avoid contamination
Degradability rate matching with re-growth rate	For gradual transfer of load-bearing and support functions to newly growing tissues
High water content	Helps in generating hydrated *in vivo* environment

Sublimation, the main principle for freeze-drying, enables the frozen water to directly pass from solid state to vapour state, without passing through the liquid state, which takes place at pressure and temperature below 4.579 mm-Hg and 0.0099 ^{o}C, respectively. In order to freeze-dry a material, it needs to be frozen first and then subjected to a high vacuum enabling the frozen liquid (e.g. water) to sublime and leave only solid and dried components of the original solution. This process leads to highly porous polymer scaffold to be used in tissue engineering approaches [15, 19-21].

Lyophilisation is performed at pressure and temperature conditions below the triple point so that the frozen liquid can sublime (Figure 1.2). Freeze-drying process starts from sample preparation and freezing to primary and secondary drying. The concentration gradient that emerges during the process between the drying front and condenser drives the removal of liquid in lyophilisation. Liquid crystals start to separate from the solution until it becomes maximally concentrated. The fundamental process steps for freeze-drying can be summarised as follows [19]:

- Freezing: The material is frozen to provide a condition for low temperature drying.
- Vacuum: After freezing, the material is placed under high vacuum to enable the frozen solvent in the solution to pass directly to vapour state (sublimation).
- Heat: Heat is applied to accelerate sublimation.
- Condensation: Condensation removes the solvent in vapour state by converting it back to a solid phase that enables the completion of lyophilisation process.

Critical features including pore size and specific pore area for scaffolds produced by freeze-drying can be optimised by adjusting some processing parameters such as pressure/temperature and duration [21, 22]. Despite its broad range of benefits, this technique may be a time- and energy-consuming approach since it requires a long time period to completely eliminate solvents [19, 20].

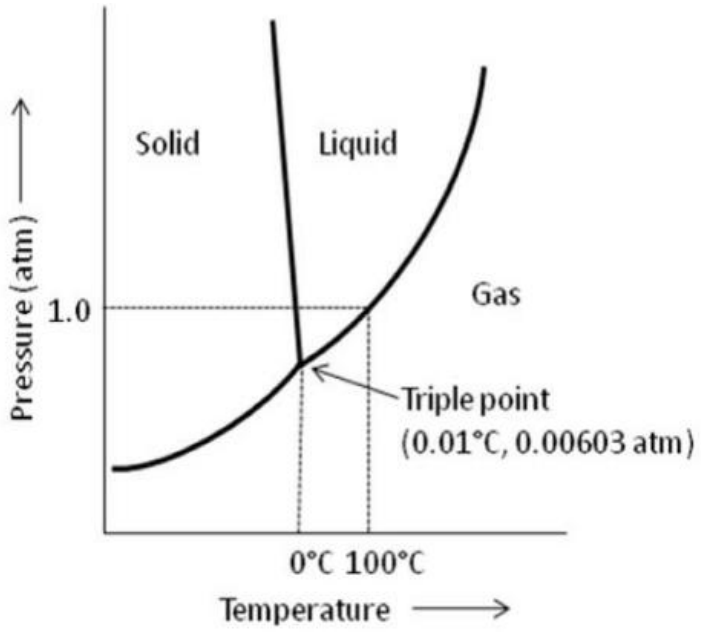

Figure 1.2: Phase diagram showing the triple point of water at 0.01 ^{o}C and 0.00603 atm [23].

1.4.2 Solvent casting and particulate leaching

Solvent-casting/particulate leaching method has been widely used to fabricate polymeric constructs with controlled porosity and surface-to-volume ratio [15, 20, 24]. In this method, a water-soluble porogen, mostly salt, sugar, paraffin or gelatin spheres, is mixed in a polymer solution and then transferred into a mold with desired shape and volume. The solvent is then removed by evaporation or freeze-drying and the porogen is leached out using its solvent, generallydeionised water [9, 20]. Adjusting porogen dimension and porogen/polymer ratio enables to construct a scaffold with desired pore size and porosity, respectively. On the other hand, loss of biomolecules in the scaffold, weak removal of porogen particles or solvent and limitation in overall size of the scaffold can be addressed among disadvantages of particulate-leaching method [20].

1.4.3 Gas foaming

The gas foaming method allows the fabrication of highly porous scaffolds in tissue engineering. To do this, a polymer solution is saturated with high pressure carbon dioxide (800 psi) forming phase separation of carbon dioxide molecules and pore nucleation (foaming) and thus eliminating organic solvent need as seen in particulate leaching method [9, 24]. These pores provide a significant increase in polymer volume and decrease in density of polymeric matrix. Three-dimensional biomimetic

construct isconsequently formed after completion of the process (Figure 1.3) [15]. However, lack of pore interconnectivity especially at the surface of newly established scaffolds makes them unsuitable for cells to be seeded [9].

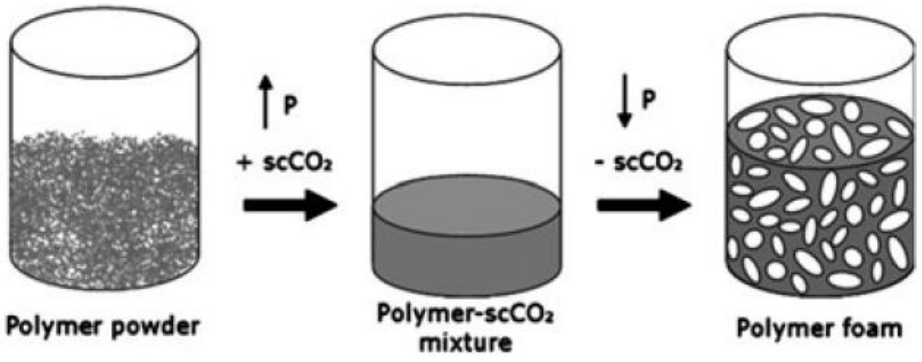

Figure 1.3: General description for gas foaming method [20].

1.4.4 Electro-Spinning

Electro-spinning method which requires high electric field was invented by Formhals in 1930s. This technique produces nanometrefibres and pores interconnected with each other that highly mimic natural extracellular matrix for cell adhesion and nutrient transportation [25-29]. When the applied electric field overcomes the surface tension, the polymer solution is ejected as jets toward collector systemand can be collected as fibres (Figure 1.4). The properties of these nanofibrescan be adjusted by changing process parameters such as viscosity and conductivity of polymer solution, voltage in the electric field, average molecular weight of polymer, distance between needles and collectors [26].

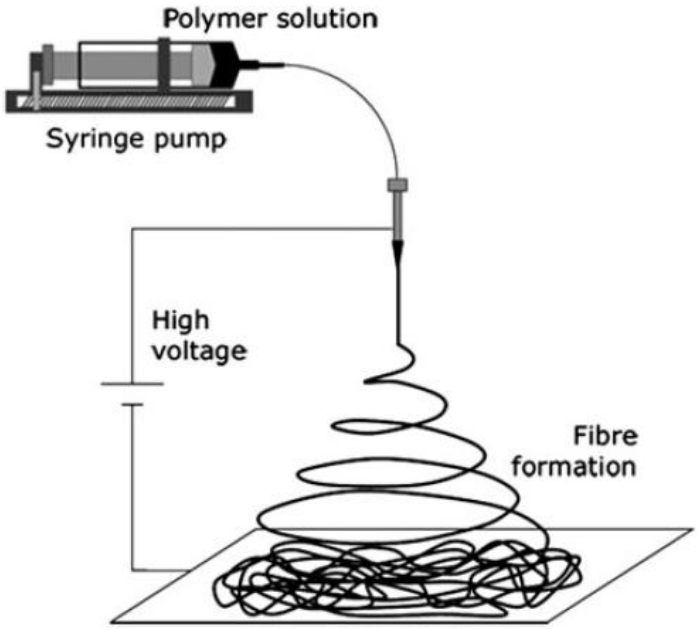

Figure 1.4: General scheme for electro-spinning method [20].

1.5 Use of Synthetic sand Natural Polymers in Tissue Engineering

In terms of tissue engineering and regenerative medicine applications, there are some important parametres to consider such as biocompatibility and reproducibility of manufacturing biomimetic materials that can be derived from nature or be synthesised in laboratory in the form of synthetic polymers, metals, alloys and ceramics [16, 30]. For this reason, increased demand for tissue engineering scaffolds has triggered an array of biomaterials in order to develop and improve methodologies that have been used [31].

Materials like polymers, metals and ceramics are widely used as cell scaffolds for tissue engineering. Synthetic and natural polymers have become the focus of many clinical trials, but each kind of polymer has its own limitations. Synthetic polymers can be easily processed and modified, whereas natural polymers provide better biocompatibility. On the other hand, different tissue types require specific physical, mechanical and degradation properties. As a result, it can be stated that there is no universal biomaterial that could meet all needs and properties of all tissues [32].

1.5.1 Synthetic polymers

The development of polymers for medical purposes has started with the need of biostable materials in order to use them during the lifetime of a patient. The first biodegradable polymer poly (glycolic acid) was used to fabricate the first, synthetic degradable suture line, ending the use of the ones made from animal intestines [33, 34].

There is an increased demand and use of synthetic biomaterials for tissue engineering approaches. The advantage of using these kinds of materials is that they are more uniform and more predictable with respect to their both chemical and mechanical properties, making it possible to meet tissue-specific needs and other requirements such as being non-toxic and bioavailable since they are not derived from animal sources [35, 36]. Changing molecular weight, co-polymer ratio and monomeric substitutions enables polymer modification for desired degradation profile associated with native tissue properties. However, there are also biomaterials that cannot be degradable, and thus, can be used to replace large tissue defects that cannot induce their own regeneration [36].

1.5.1.1 Non-Biodegradable synthetic solymers

Non-biodegradable synthetic polymers are mainly used in dental tissue engineering. However, problems due to infection and capsule formation around these biomaterials and the need for a second operation to remove them make their use disadvantageous for tissue engineering [36].

1.5.1.2 Biodegradable synthetic polymers

Because of their physical properties, cost-effectiveness and low immune response in host tissues, synthetic polymers possess many advantages in order to be used to establish scaffolds for bone tissue regeneration [36].

Polyesters

Polyesters, which are composed of ester linkage backbones and degraded by hydrolysis *in vivo*, are important biodegradable synthetic polymers. Important examples include poly (glycolide) (PGA), poly (lactide) (PLA), poly (caprolactone) (PCL), and poly (trimethylene carbonate) (PTMC). Due to their almost non-toxic degradation products, polyesters are extensively used to produce scaffolds.

Additionally, they are degraded by bulk erosion or surface erosion totally, resulting in controlled release of degradation products or other materials such as drugs for which they are used as delivery vehicles [36].

Poly (Ether-Ester)

As a poly (ether-ester), poly (dioxanone) (PDS) is used in important biomedical applications since it possesses enhanced flexibility making it useful especially in esophageal dilation and vascular grafting. It is degraded by hydrolysis completely up to six months [36].

Poly (Ethylene Glycol)

Poly (ethylene glycol) (PEG) composed of repeating ethylene oxide monomeric subunits is a highly utilised polymer with specific properties such as solubility in organic and hydrophilic solvents. PEG is used to create less hydrophobic polymers, making cell adhesion and proliferation on scaffolds possible [36].

1.5.2 Natural polymers

Proteins and polysaccharides as natural polymers are being widely used and, based on their diverse chemical and physical properties, they play an important role in tissue engineering applications [35].

1.5.2.1 Proteins

Materials made from proteins are useful in biomedical applications since they are the major components of natural tissues and display a well-controlled natural degradation profile (Table 1.2) [35].

Collagen

Collagen is an ECM protein, which is abundantly found in musculoskeletal tissues. There are approximately 22 different types of collagen proteins, and they can be extracted from animals such as rats, bovines and humans. By making use of collagen in different concentrations, features of a scaffold can be adjusted accordingly. Some studies already demonstrated collagen possesses similar physical and mechanical properties to those of natural tissues and provides a better cell adhesion and growth *in vitro*. Collagen scaffolds can be designed as tubes, sponges, powders and sheets,

and are used in muscle, cardiovascular, skin, cartilage, tendon and ligament tissue engineering approaches (Figure 1.5) [35].

Figure 1.5: Examples for some commercially available collagen scaffolds [35].

Gelatin

Gelatin is a hydrolysed protein form of collagen obtained by denaturing its triple-helix structure into single-stranded molecules [37-40]. For gelatin extraction, collagen molecules are obtained from bovine or porcine skin or bone as a by-product of meat-processing industry. Extracts from collagen are derived under either acidic or basic conditions, and referred to as type A or type B gelatin, respectively [41].

Gelatin is an interesting and important polymer for tissue engineering applications. It promotes cell attachment, proliferation and differentiation, and due to its biodegradability, biocompatibility and low cost, is used in many applications in the pharmaceutical, medical and food industries [35, 39, 42].

Gelatinhas been used generally in combination with other materials in order to form scaffolds since it possesses low mechanical properties on its own [37]. To use gelatin as a biomaterial, its instability issue can be overcome by covalent cross-linking methods either without prior modification or after functionalisation of its side groups [41].

Gelatin has both acidic and basic functional groups that enable its chemical modification with other polymers [37]. Importantly, even after hydrolysis from collagen, gelatin retains its bioactive sequences (e.g. the arginine-glycine-aspartic acid (RGD) peptide) for cell attachment in its backbone [41].

Elastin

Elastin is an extracellular matrix protein and found abundantly in tissue where elasticity is of great importance. The ratio of elastin in blood vessels, elastic

ligaments, lungs and skin is 50%, 70%, 30% and 2-4% of their dry weights, respectively. Associated with a wide range of elastic peptide and protein sequences existing in different lengths and compositions, elastin is not a single, well-defined, but a rich molecule in glycine, proline and lysine [33].

Because of causing calcium-rich precipitates when used in heartvalve prosthetic devices and preventing cells attachment and growth on its surface, elastin serves as an important example showing that using natural polymers is not a guarantee for clinically successful tissue engineering applications [33].

Keratin

Keratin, a fibrous protein found abundantly in nature, is the main constituent of hair, wool, nail, horn and hooves of mammals, birds and reptiles [43-44]. It contains cysteine amino acid residues (7-20%), the oxidation of which leads to intermolecular and intramolecular covalent bonds responsible for the tough keratin fibres [43].

Its cell adhesion sequences RGD, arginine-glycine-aspartic acid, and LVD, leucine-asparagine-valine found in natural extracellular matrix proteins and cellular binding motifs that mimic cellular attachment sites make keratin proteins useful for the development of various tissue engineering scaffolds [43]. Like many other natural biomaterials, it possesses unique biological activities and biocompatibility [44].

Silk

Silk fibres have been widely used in people's daily life as a product from textile industry and also as an FDA-approved biomaterial for biomedical purposes such as human-made blood vessels, surgical sutures and repair materials due to its high oxygen permeability, biocompatibility, controllable biodegradability and excellent mechanical properties [45-50]. In tissue engineering applications, scaffolds produced from silks by salt-leaching, freeze-drying, gas foaming or electro-spinning techniques provide supporting constructs for cells including fibroblasts, osteoblasts, hepatocytes and stem cells [45].

Silk protein secreted by *Bombyxmori*silk worm consists of fibroin and sericin [51]. The silk fibroin is present within silk worm cocoons as a double-stranded fibre, which is coated with glue-like protein, called sericin. The raw silk fibre mass is composed of about 20-30% sericin and 70-80% fibroin with a very low amount of waxes and carbohydrates. Pure silk fibroin protein is prepared by a degumming

procedure and thus separated from the sericin protein since sericin may cause inflammatory responses [52-54].

Silk fibroin consists of a heavy protein chain with approximately 390 kDa molecular weight and a light protein chain with approximately 26 kDa molecular weight connected by a disulfide bond. The heavy chain of silk fibroin is composed of a block co-polymer arrangement of primarily hydrophobic amino acids and is the source for robust mechanical properties, whereas the light chain consists of about 47% hydrophobic amino acid residues and is crucial for proper cellular secretion of the heavy chain (Figure 1.6). The amino acid sequence of silk fibroin heavy chain mainly consists of Gly-X repeats where X refers to alanine, serine or tyrosine [52, 55-57].

Silk fibroin can exist in three different structural morphologies as silk I, silk II and silk III. Silk I form is water-soluble, whereas silk II is an insoluble form consisting of extended anti-parallel β-sheets stabilised by hydrogen bonding. The silk III is helical and observed at the air-water interface [52, 55, 58].

Sericin proteins have a molecular weight ranging from 20 to 400 kDa depending on gene coding and post-translational modifications. The primary amino acid sequence of most sericins contains a repeat of 38 amino acids composed of serine, glycine, asparagine, aspartic acid, and a random coil secondary structure [52].

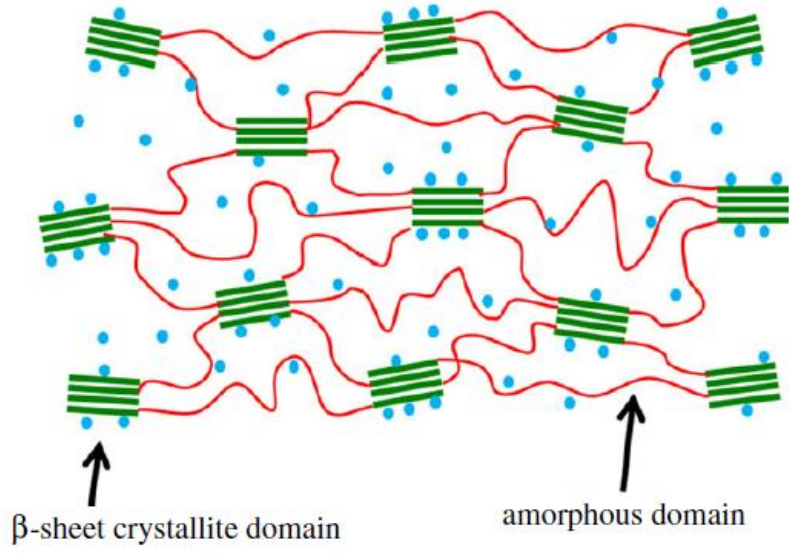

Figure 1.6: The hydrophobic β-sheet structure of silk fibroin embedded in the amorphous regions, which are hydrophilic and hold moisture (water molecules are shown by blue dots) [55].

Proteoglycans

Proteoglycans, PGs, consisting of one or more glycosaminoglycan (GAG) chains attached to serine residues within a core protein are major components of extracellular matrix. They show great structural diversity since a PG may contain various GAG chains in type, number and length with a different core protein than other PGs. The core protein and GAG chains of a proteoglycan play significant roles in tissue remodelling, intracellular signalling, protein uptake, cell migration and other critical functions of natural tissues. Therefore, these proteins are in specific interest to many researchers for tissue regeneration techniques and can be introduced onto the surface of biomimetic constructs, used alone or in combination with other matrix proteins such as fibrin, collagen to create more bioavailable materials with appropriate biological and physical properties [33].

Table 1.2: Biodegradable natural polymers and their properties [34].

Type of protein	Source of protein	Function of protein
Collagen	Isolated from cattle, fish, and other species	Key component of tissue architecture, provides mechanical strength, supports cell attachment and growth, and provides a biocompatible matrix for cell transplantation. Used extensively as a tissue expander and bulking agent in cosmetic products.
Gelatin	Partially hydrolized collagen	Used in food industry, widely explored by researchers as a matrix for three-dimensional cell culture and as a component of tissue-engineering scaffolds.
Elastin	Isolated from elastic tissues of cattle and birds	Key component of tissue architecture, provides elasticity to tissues.
Keratin	Isolated from skin, hair and nails of cattle and birds	Key structural component of outer skin, hair and nails.Used as a matrix for cell growth and as a component in wound dressings and skin care products.
Silk	Isolated from insect larvae	Used in the textile industry because of its extraordinary strength. Also studied as a component of tissue engineering scaffolds and as a cell culture substrate.
Proteoglycans	Various tissue extracts	Used in research of cell-matrix interactions, matrix-matrix interactions, cell proliferation, cell migration.

1.5.2.2 Polysaccharides

Polysaccharides are long carbohydrate molecules that contain repeated monosaccharide units bound with each other by glycosidic bonds, and form the second largest biopolymer class of extracellular matrix, where some glycosaminoglycans like hyaluronic acid (HA) and chondroitin sulphate (CS) comprising repeating disaccharide units are present (Table 1.3) [59]. Hyaluronic acid is the most prominent glycosaminoglycan with responsibility for *in vivo* regulation of the water content of natural tissues and contributing to the viscoelastic behaviour of cartilage tissue. It can also promote angiogenesis [59].

Cellulose

Mainly found in cell walls of plants, cellulose is a tough, water-insoluble, fibrous material composed of D-glucose units linked together by glycosidic bonds. Despite its some disadvantages as a biomaterial such as being non-biodegradable in humans because of lack of specific digestive enzymes, cellulose is being commercially used in paper, wood and textile industries. Apart from the molecule itself, some cellulose derivatives such as methylcellulose, hydroxyl propyl cellulose and carboxymethylcellulose are used as drug delivery agents, barrier for preventing surgical adhesion or even fabricating scaffolds for cartilage tissue engineering [33].

Starch

Starch is also composed of D-glucose units bound together by different glycosidic bonds than in cellulose, making it digestible and thus useful as an important human nutrient. Linear and branched chains named amylose and amylopectin, respectively, are found in starch and their proportion in the molecule dictates whether it can be totally water-insoluble or partially soluble at room temperature [33].

Starch is not an obvious option for tissue engineering applications since it is not biodegradable in human tissues even though it can be digested in the gut. However, some polymers consisting of starch molecules can display biodegradable and biocompatible properties, and therefore can be used in cartilage tissue regeneration approaches and as drug delivery agents [33].

Alginate

Alginates are anionic polysaccharides and binary copolymers of L-guluronic acid (G monomer) and D-mannuronic acid (M monomer). The ratio of these two monomers in alginate polymers depends on the type and growing season of the source seaweeds that may have a negative impact for the production of materials with same or comparable properties. The proportion and distribution together can also affect the physiochemical properties of the polymer since cells to be attached onto the scaffolds made from alginate molecules will be sensitive to local and natural differences of the biomaterial. Like other natural polymers, the purity of alginate needs to be evaluated to prevent contamination caused by endotoxins, heavy metals and other impurities [60].

Glycosaaminoglycans

Glycosaminoglycans (GAGs) consisting of repeating disaccharide units usually include auronic acid component such as glucuronic acid and a hexosamine component such as N-acetyl-D-glucosamine. Chondroitin sulphate, dermatan sulphate, keratansulphate and heparansulphate are the predominant GAG types attached to proteoglycan core proteins by specific carbohydrate sequences containing three or four monosaccharides [33].

Hyaluronic acid (HA), the largest GAG molecule, can be easily chemically modified in order to yield an appropriate biomaterial for various biomedical applications. It is not an antigenic material and does not provoke an immune response. In addition, hyaluronic acid is a desirable material in medical device developments and has been used as a viscoelastic in eye surgery since 1976 since it can be easily isolated and modified. The benzyl ester of HA is also being studied for use in vascular grafts [33].

Chitin/Chitosan

Chitosan is a natural, cationic, non-antigenic, biocompatible and biodegradable amino-containing polymer that is derived from chitin through a partial deacetylation process that has a similar structure to the naturally present glycosaminoglycans in extracellular matrix, and consists of D-glucosamine and N-acetyl-D-glucosamine units [61-66]. Because of its cationic nature, chitosan is also bioadhesive, haemostatic and antimicrobial, and bind and prolong the activity of growth factors that promote cell-cell and cell-matrix interactions [66]. The chemical and mechanical

structure of chitosan can be easily modified to generate materials with novel properties and functions [67]. For this reason, it is widely used for drug delivery, wound dressing and tissue engineering applications [66]. On the other hand, similar to gelatin, it possesses low mechanical strength and a high biodegradation rate [62].

Table 1.3: Biodegradable and widely used natural polysaccharides and their properties [34].

Type of polysaccharide	Source of polysaccharide	Function of polysaccharide
Cellulose	Cell wall of green plants	Main structural component of plants which keeps the stems, stalks and trunks rigid
Type of polysaccharide	Source of polysaccharide	Function of polysaccharide
Starch (Amylose and Amylopectin)	Present in all staple foods	Important in plant energy storage
Alginate	Found in the cell walls of bacteria	Protects bacteria from engulfment by predatory protozoa or white blood cells (phagocytes)
Glycosaaminoglycans	Widely distributed	Cell-matrix interactions, matrix-matrix interactions, cell proliferation, cell migration
Chitin/Chitosan	Major component of the exoskeleton of insects, shells of crustaceans, cell walls of fungi	Structural component

1.6 Non-polymeric Materials

1.6.1 Ceramics

Apart from the polymers, most prominent materials used in bone tissue engineering applications are ceramics because of their mechanical and structural advantages. Many of them, such as hydroxyapatite-based ceramics, are not biodegradable, but do still have an advantegous position in large bone defects' replacement. Some ceramics like tri-calcium phosphate and calcium carbonate can be degraded *in vivo*, but preferred for repairing small defects in bone tissues [36].

1.6.2 Bioactive glass

Bioactive glass is generally used in combination with ceramic materials due to its ability to promote in vivo tissue adhesion. It can initiate hydroxyl carbonate apatite

coating on its surface that is similar to hydroxyapatite particles in bone tissues. The interaction between these minerals allows the scaffold to adhere to the bone. In addition, bioactive glass can also be used as delivery molecules for therapeutically relevant drugs to reach the site of regeneration [36].

1.7 Bone Tissue Regeneration

1.7.1 Bone tissue structure

Natural bone consisting of both inorganic minerals and biomacromolecules is a highly functionalised connective tissue that forms the skeletal framework of human body due to its cellular and structural organisation and component material properties directing its own formation (Figure 1.7) [64, 68, 69]. The biomacromolecules of bone tissue are mainly collagen fibrils that provide strength and resistance, and the inorganic minerals are mainly hydroxyapatite (HA) molecules that resist compression and crystallisealong the collagen fibril axis [64, 70].

The organic part of bone tissue makes its 35%, whereas the rest is made of inorganic matrix consisting of hydroxyapatite as well as carbonate and inorganic salts. The organic extracellular matrix of natural bone tissue is composed of complex and self-assembled molecules such as collagen, which makes up approximately 90-95% of the organic ECM, and osteopontin, osteonectin, osteocalcin, bone sialoprotein, hyaluronan and proteoglycans [71].

The overall bone structure is divided into two different subgroups: the cortical bone, which is more compact, and the cancellous bone appearing like a sponge and possessing pore filled with bone marrow or fat [71]. Bone tissue is continuously renewed and remodelled by formation and resorption of bone-forming osteoblasts and bone-resorbing osteoclasts to adopt to mechanical loads, hormones, cytokines and other external physical parameters [69, 71].

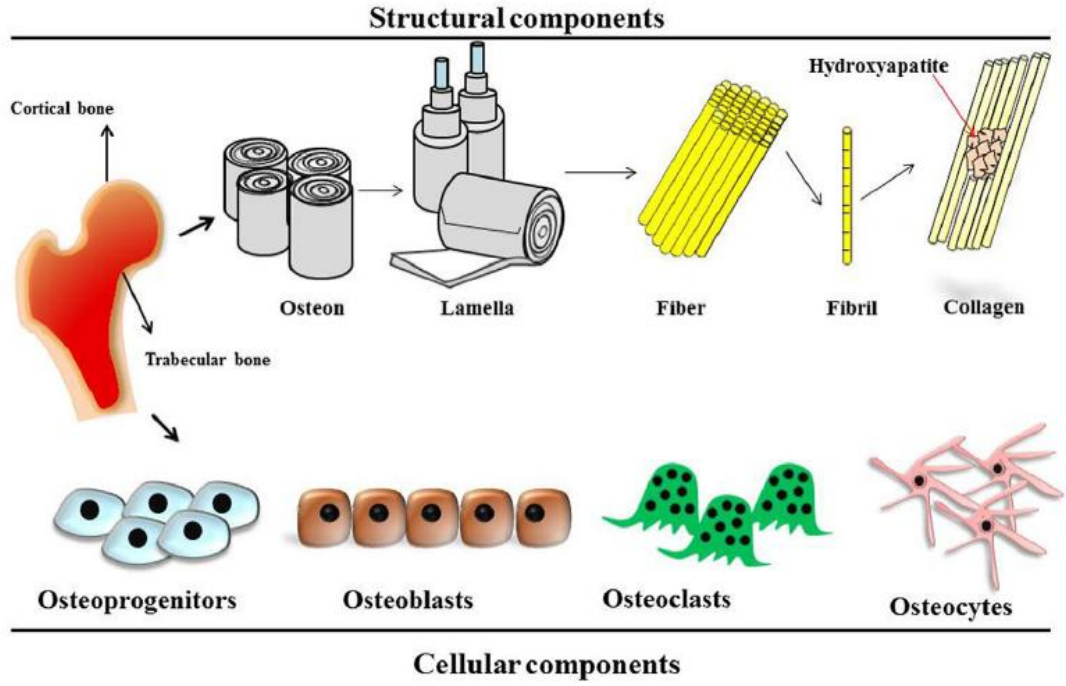

Figure 1.7: The structure of natural bone tissue showing structural and cellular components [69].

The osteocytes comprising more than 90% of all bone tissue cells in adult animals are believed to be the main cellular responsible unit for the transduction of physiological and mechanical mediators for differential cellular and tissue responses by cell-cell or cell-ECM interactions [68, 71].

Osteoclast cells, derived from hematopoietic stem cells, dissolve hydroxyapatite molecules by releasing hydrochloric acid and a protease mixture degrading the organic bone matrix in collagen fibres. They are involved in removing cracks and can also serve as immune cells by secreting cytokines that are able to affect the cells in the environment [71].

Another type of bone tissue cells, osteoblasts, is derived from mesenchymal stem cells that are located in the bone marrow serving as a valuable cell source for tissue generation through differentiation towards osteogenic lineage. After they are encapsulated within their own matrix, they gain a different morphology and become osteocytes [71].

1.7.2 Bone tissue regeneration approaches

Bone fractures have the ability to heal by themselves within a couple of weeks. Large or critical bone defects that occur because of tumour, birth defects, accidents, aging,

infection or other physiological reasons may need major important surgical interventions since they heal relatively slowly or not at all [59, 68, 69]. Such critical defects of bone tissue are treated by transplantation of autogenic (patient's own tissues) or allogenic (tissues from other patient(s)) cancellous bone grafts or by application of growth factors such as bone morphogenic protein, BMP-2, or a combination of these methods [59]. According to a report published in the US, each year 1.3 million people undergo a bone graft surgery [72].

Possible second site damages, additional pain, longer healing time for the defected site, limited supplyanddonor availability, disease transmission and infection risk need to be taken into consideration as existing disadvantages of autograft or allograft tissue transplantation [70, 72]. These limitations can be circumvented by application of a scaffold structure with desired shape and size in order to treat and/or replace damaged or diseased bone tissues. These scaffolds can be cell-free or pre-seeded with cells either from patient's own tissues or from bone tissues of a donor. In any case of these two approaches, the cells can differentiate and proliferate within the entire scaffold structure and take over the functions of target tissue with time [72].

1.7.3 Bone tissue engineering

Bone tissue engineering is a promising alternative to currently available treatments in order to regenerate bone tissue defects as it encompasses bone biology and engineering principles by making use of biomimetic scaffolds [69, 71]. Various biocompatible polymers, natural or synthetic polymers, have been studied for tissue engineering applications to produce scaffolds for bone tissue regeneration [64].

An ideal scaffold must have some important properties such as biocompatibility, osteoconductivity, good mechanical integrity, bioactivity, a degradation rate matching with the formation rate of new tissue at the site of damage and interconnected porous structure [70]. Natural polymers such as chitosan, collagen, cellulose, gelatin and silk fibroin are preferred over synthetic polymers since the natural polymers possess better biodegradability, non-toxicity, biosecurity and biocompatibility [64]. Among natural polymers, silk fibroin has been shown to be a promising biomaterial due to biological and mechanical features it provides [71].

In a study published in 2014, Orlova *et. al.* studied porous silk fibroin and silk fibroin/ gelatincomposite sceffolds produced by freeze-drying method and tried to

find out how the gelatin content in composite scaffold affects the scaffold properties. For this reason, they produced various silk fibroin scaffolds with 10, 20, 30, 40 and 50% gelatin content, and examined scaffold integrity, elasticity, cell proliferation, adhesion and migration. According to their findings, the samples with 40% and 50% gelatin content lost their structural integrity after aweek of incubation in water. All samples were elastically deformedby direct mechanical pressure, and increasing gelatin ratio resulted in increased lost in scaffold elasticity. On the other hand, addition of gelatin to the scaffold increased cell adhesion and accelarated cell proliferation [4].

In another study published by Damrongsakkul *et. al.* in 2013, the researchers modified human cancellous bone with silk fibroin/gelatin blend. For this purpose, they studied silk fibroin-gelatin solutions at a weight ratio of 50/50 with solution concentrations 1, 2 and 4 w/v%. Based on their results, all bone scaffolds modified with the blend showed smaller pore size, less porosity and lower compressive modulus when compared with unmodified human cancellous bone structure. The scaffolds modified with 2 and 4 w/v % solution concentrations stimulated cell attachment, proliferation and osteogenic differentiation of mesenchymal stem cells derived from bone marrow in comparison to the original cancellous bone [14].

Kaplan *et. al.* designed a green process, avoiding the use of organic solvents and chemical processes, to produce silk fibroin-based scaffolds for tissue engineering applications. According to their results published in 2010, addition of gelatin to the silk fibroin solution changed the conformation of silk fibroin and its interaction with water. They also showed that the pore sizes of silk fibroin-based scaffolds can be controlled by adjusting polymer ratios in blend solutions, and silk fibroin-gelatin scaffolds improved fibroblast cell interaction in *in vitro* cell culture tests [45].

2. MATERIALS AND METHODS

2.1 Materials

2.1.1 Chemicals

The list of chemicals that were used in this study and their suppliers were given in Appendix A. The gelatin was also listed in Appendix A.

2.1.2 Solutions

The solutions that were used in this study and their compositions were given in Appendix B and Appendix C.

2.1.3 Laboratory equipment

The laboratory equipment that were used in this study was listed in Appendix D.

2.2 Methods

2.2.1 Fibroin extraction from *Bombyx mori* silkworm cocoons

The silk fibroin used in this study was extracted according to a process from Rockwood *et. al.* [74]. The process consisted of following steps:

1. A 2 litres glass beaker filled with 2 litres of ultrapure water was prepared, covered with aluminium foil and then heated until boiling.
2. Meanwhile, silkworm cocoons were cut into smaller pieces of 5 g weight.
3. Sodium carbonate (4.24 g) was added to the water and completely dissolved.
4. The cocoon pieces were added to the boiled water and cooked for 30 minutes. It was occasionally stirred with a spatula to promote good dispersion of fibroin.
5. The silk fibroin was removed and then cooled in ultrapure water. The excess water was squeezed out of the silk, and the sodium carbonate solution in the silk was discarded.

6. The fibroin was put into a 1 litre beaker filled with 1 litre of ultrapure water and a stir bar.
7. The fibroin was rinsed in water changed for every hour while gently stirring on a stir plate.
8. The steps 6 and 7 were repeated for a total of three times.
9. After the third wash, the silk was removed, squeezed well, and then spread out on a clean aluminium foil.
10. The amount of 9.3 M lithium bromide needed to make a 20 w/v % solution based on the amount of dried silk fibroin was calculated and prepared according to Equation 2.1. Since silk to LiBr should be 1 to 4, the amount of the dried silk fibroin was multiplied by 4 to get the total volume of 9.3 LiBr needed.

$$(86.85\ \frac{g}{mol})\ (9.3\ \frac{mol}{L})(\frac{1L}{1000\ mL})\ (X)= g\ of\ LiBr \qquad (2.1)$$

11. The silk fibroin was packed tightly into a 50 mL glass beaker, and the required amount of LiBr solution was added on top.
12. The fibroin was dissolved in an oven at 60 ^{o}C for overnight.
13. The dialysis cassettes were hydrated in water for a few minutes.
14. 12 mL of the silk fibroin-LiBr solution was inserted into a 3-12 mL dialysis cassette with the help of a 20 mL syringe.
15. Dialysis against 1 litre of ultrapure water per 12 mL cassette was performed. To ensure mixing, a large stir bar was used. The water was changed every three hours for three times a day for 2 days (6 changes within 48 hours).
16. The silk fibroin was removed from the dialysis cassettes with another syringe, splitted into three 15 mL conical tubes. A tube filled with water was used for counterbalance.
17. Centrifugation was performed at 9,000 rpm at 4 ^{o}C for 20 minutes to remove impurities.
18. The tubes were removed from the centrifuge carefully. The silk was transferred into another tube.
19. The steps 17 and 18 were repeated.
20. In order to determine the silk fibroin concentration, 1 mL of the silk fibroin solution was weighed and dried in an oven at 60 ^{o}C overnight. The dried silk

fibroin was weighed and the yield of the solution in percentage was calculated according to Equation 2.2.

$$\frac{\text{(The dried weight of silk fibroin - the wet weight of silk fibroin)}}{\text{The wet weight of silk fibroin}} \text{x}100 \quad (2.2)$$

2.2.2 Preparation of silk fibroin-gelatin blend solutions

Silk fibroin was extracted from *Bombyx mori* silkworm cocoons according to a process that had been adopted from Rockwood *et. al* (Section 2.2.1) [74]. The gelatin from bovine skin Type B was commercially purchased (Appendix A).

A stock gelatin solution with 4% (w/v) concentration was prepared by dissolving powdered gelatin in ultrapure water with the help of a magnetic stirrer at 60 ^{o}C for approximately half an hour. As a cross-linking agent for gelatin polymer, glutaraldehyde solution with 1% (w/v) concentration was added into the stock gelatin solution at a ratio of 1:32 (v/v), as adopted from Yang *et. al*. and mixed with the help of a magnetic stirrer at 60 ^{o}C for 15 minutes (Appendix A) [3]. The stock gelatin solution was then splitted into different beakers and diluted to 1% (w/v), 2% (w/v) and 3% (w/v) in order to prepare silk fibroin-gelatin blend solutions.

After the extraction process, a stock silk fibroin solution of 5.8% (w/v) was yielded. The stock solution was then transferred into different beakers and diluted to 3% (w/v), 2% (w/v) and 1% (w/v) in order to prepare silk fibroin-gelatin blend solutions.

Once the stock solutions were prepared and then diluted to desired concentrations, the corresponding silk fibroin and gelatin solutions were mixed at a ratio of 1:1 (v/v). To do so, the diluted silk fibroin solutions were added into the gelatin solutions with appropriate concntrations and were gently mixed with the help of a magnetic stirrer at approximately 40 ^{o}C for half an hour. Totally, five different blend solutions were prepared with total polymer concentration of 4% (w/v). The compositions of these solutions were described in Table 2.1. The solution were named after the weight to volume ratios of each component in the blend. The “F” and “G” represented silk fibroin and gelatin, respectively.

The blend solutions were cooled at 4 ^{o}C for 24 hours and then frozen at -20 ^{o}C until lyophilisation, as adopted from Yang *et. al.* [3].

Table 2.1: Compositions of silk fibroin-gelatin blend solutions.

	Silk Fibroin Content (% w/v)	Gelatin Content (% w/v)	Total Polymer Content (% w/v)
F4-G0	4	0	4
F3-G1	3	1	4
F2-G2	2	2	4
F1-G3	1	3	4
F0-G4	0	4	4

2.2.3 Lyophilisation of silk fibroin-gelatin blend solutions

The frozen silk fibroin-gelation solutions were lyophilised with the help of a freeze-dryer (Appendix D). The freeze-drying parametres were -55 ^{o}C and 24 hours for main drying step and -30 ^{o}C and 1 hour for final drying step. Following lyophilisation process, the freeze-dried samples were treated with an aqueous solution of 99% methanol for half an hour and dried in a vacuum hood for an additional half an hour, as adopted from Chomchalao *et. al.* [11] (Appendix A). The amount of methanol was calculated based on the weight of silk fibroin polymer in the blend solution. For 1.7 g of silk fibroin, 1 mL of 99% methanol was used [74]. The methanol treatment enabled water-insoluble silk fibroin polymer through β-sheet formation. The samples were then kept in a desiccator.

2.2.4 Characterisation of silk fibroin-gelatin composite scaffolds

2.2.4.1 Analysis with scanning electron microscopy

The porosity and surface morphology of composite scaffolds were examined by Scanning Electron Microscope (Appendix D). The surfaces of samples were scanned at approximately 100x magnification.

2.2.4.2 Analysis with fourier transform infrared spectroscopy

Fourier transform infrared (FTIR) spectra of freeze-dried composite scaffolds were taken in order to examine the secondary structures of the silk fibroin-gelatin sponges (Appendix D).

2.2.5 Water-uptake test of silk fibroin-gelatin composite scaffolds

The water-uptake test for F3-G1, F2-G2 and F1-G3 composite scaffolds was performed based on a process that had been adopted from Lerdchai *et. al.* [75]. First, dry samples were weighed (W_d) and then immersed in phosphate buffered saline

solution (0.01 M, pH 7.4) at 37 ^{o}C for 24 hours (Appendix B). After that, the excessive water was removed from the sample surfaces and the swollen samples were weighed (W_s). The percentage of water absorbed by samples was calculated according to the Equation 2.3. The test was repeated for three samples of each composite scaffolds and their average percentage was calculated.

$$\text{Water-uptake ratio (\%)} = \frac{W_s - W_d}{W_d} \text{x} 100 \tag{2.3}$$

2.2.6 3-day biodegradation test of silk fibroin-gelatin composite scaffolds

A three-day *in vitro* biodegradation test for F3-G1, F2-G2 and F1-G3 composite scaffolds was performed to determine an optimum enzyme concentration for the main biodegradation assay that lasted 28 days.

Three enzyme solutions with different concentrations were prepared from powdered Protease XIV (from *Streptomyces griseus* with 3.5 units/mg, Appendix A). First, a stock enzyme solution with 1 U/mL concentration was prepared according to the Equation 2.4. The amount of powdered Protease XIV enzyme was dependent on the volume of stock enzyme solution. For instance, for an enzyme solution with 15 mL volume and 1U/mL concentration, 4.29 mg of enzyme powder was dissolved in PBS (pH 7.4) at room temperature.

$$\text{Enzyme concentration (U/mL)} = \frac{3.5 \text{ units}}{\text{mg}} \text{x} \frac{\text{mg}}{\text{mL}} \tag{2.4}$$

The stock enzyme solution was stored at -20 ^{o}C. The stock solution was transferred into different conical centrifuge tubes and diluted with PBS (pH 7.4) to prepare enzyme solutions with 0.05, 0.1 and 0.2 U/mL concentrations. As adopted from a study of Lerdchai *et. al.*, sodium azide was added to the enzyme solution at a ratio of 0.01% at room temperature (w/v) in order to prevent microbial growth around the samples (Appendix A) [75]. The dry weight (W_i) of F3-G1, F2-G2 and F1-G3 composite scaffolds were calculated. Then, the samples were immersed separately in each enzyme solution and incubated at 37 ^{o}C for three days. After that, the samples were freeze-dried and weighed (W_f). Freeze-drying parametres were -55 ^{o}C and 24 hours for main drying step and -30 ^{o}C and 1 hour for final drying step. The remaining weight ratio of samples were calculated based on Equation 2.5. The test was repeated

for three samples of each composite scaffold and their average was calculated. The control samples were immersed in PBS solution (pH 7.4) that contained no protease enzyme and sodium azide.

$$\text{Remaining weight ratio (\%)} = \frac{W_f}{W_i} \times 100 \qquad (2.5)$$

2.2.7 Biodegradation test of silk fibroin-gelatin composite scaffolds

The main *in vitro* biodegradation test that lasted 28 days was conducted by using a Protease Type XIV enzyme solution of 0.05 U/mL for F3-G1 and F2-G2 composite scaffolds. The enzyme solution was prepared as previously described in Section 2.2.5 [75]. The control samples were immersed in PBS solution (pH 7.4) that contained no protease enzyme and sodium azide.

The test was adopted from Teimouri *et. al.* [5] and Lerdchai *et. al.* [75]. First, the samples were weighed (W_i) and then placed into 12-well plates in which they were immersed in Protease XIV enzyme solution and incubated at 37 ^{o}C for different time intervals of 7, 14, 21 and 28 days. The enzyme solution was replaced with fresh enzyme solution that had been prepared from the stock enzyme solution every 2 days to enable continuous enzymatic activity. After each time period, the corresponding samples were taken out, the excessive enzyme solution was removed and the samples were freeze-dried. The freeze-drying parametres were -55 ^{o}C and 24 hours for main drying step and -30 ^{o}C and 1 hour for final drying step. After that, the freeze-dried samples were weighed (W_f) and the percentage of remaining sample weight was calculated according to the Equation 2.3.

The samples were visualised after biodegradation study by scanning electron microscope at approximately 60x magnification.

2.2.8 Biomineralisation test of silk fibroin-gelatin composite scaffolds

The *in vitro* biomineralisation test was conducted for F3-G1 and F2-G2 composite scaffolds, as adopted from Teimouri *et. al.* [5]. The samples were placed into 12-well plates, immersed either in 1x modified simulated body fluid or in 3x modified simulated body fluid solutions and then incubated at 37 ^{o}C for different time intervals of 1 day, 4 days and 7 days. The modified simulated body fluid (mSBF) solutions were prepared as described in Appendix C [73]. For samples that were incubated for

7 days, the mSBF solution was replaced with fresh solution at the end of the 4th day of the test. After each time period, the corresponding samples were taken out, rinsed two times with ultrapure water to remove adsorbed minerals and freeze-dried. The freeze-drying parametres were -55 ^{o}C and 24 hours for main drying step and -30 ^{o}C and 1 hour for final drying step. After that, the samples were examined by scanning electron microscopy and fourier transform infrared spectroscopy to determine whether hydroxyapatite crystals were formed on scaffold surface.

3. RESULTS AND DISCUSSION

3.1 Characterisation of Scaffolds

3.1.1 Morphology of scaffolds

The presence and overall distribution of pores on scaffolds' surfaces were determined by scanning electron microscope images that were given in Figure 3.1. When all silk fibroin-gelatin composite scaffolds were examined, it could be seen that F2-G2 (Figure 3.1b) and F1-G3 (Figure 3.1c) samples showed better and uniform surface porosity and homogenous pore distribution. For scaffolds consisting of only one polymer, the one constructed with gelatin, F0-G4 (Figure 3.1e) seemed to have a relatively porous surface structure when compared to the one prepared from only silk fibroin (Figure 3.1a). The F4-G0 samples formed distinct layers instead of porous structures. The SEM images of F4-G0, F3-G1, F2-G2, F1-G3 and F0-G4 samples showed that increasing the gelatin content in silk fibroin-gelatin blend solutions led to decreased layer formation and more porous scaffold structures. Pore formation was more apparent for samples that contained the gelatin polymer above 50% of total polymer blend.

The SEM images and porosity analysis results obtained in this study were consistent with the results previously reported by some researchers. Lu *et. al.* showed that addition of gelatin to aqeuous silk fibroin solution changed the silk fibroin conformation and silk fibroin-water interactions by affecting hydrophilic interactions between silk fibroin, gelatin and water and prevented formation of separate layers. According to their results, the gelatin content above 20% of total silk fibroin-gelatin blend provided more and more porous scaffolds [45].

In another study published by He *et. al.* in 2012, the researchers showed that increasing gelatin content in silk fibroin-gelatin blends gradually changed the morphology of silk fibroin-gelatin scaffolds from lamellar to porous structure [49].

In a recent study, Lerdchai *et. al.* observed a homogenous porous structure and interconnected pores when they examined the morphology of silk fibroin-gelatin

scaffolds. They also showed that the porosity of silk fibroin-gelatin composite scaffolds increased as the gelatin content in the scaffolds was increasing [75].

The morphologies obtained in this study were in consistency with the results of other studies that were previously reported. It can be concluded that increasing gelatin content in silk fibroin-gelatin composite scaffolds reduced separate layer formation and formed more and more homogenous porous scaffold structure.

Based on these results, F3-G1, F2-G2 and F1-G3 samples were selected for water-uptake and 3-day *in vitro* biodegradation tests because of their homogeneous porous structures and overall morphologies.

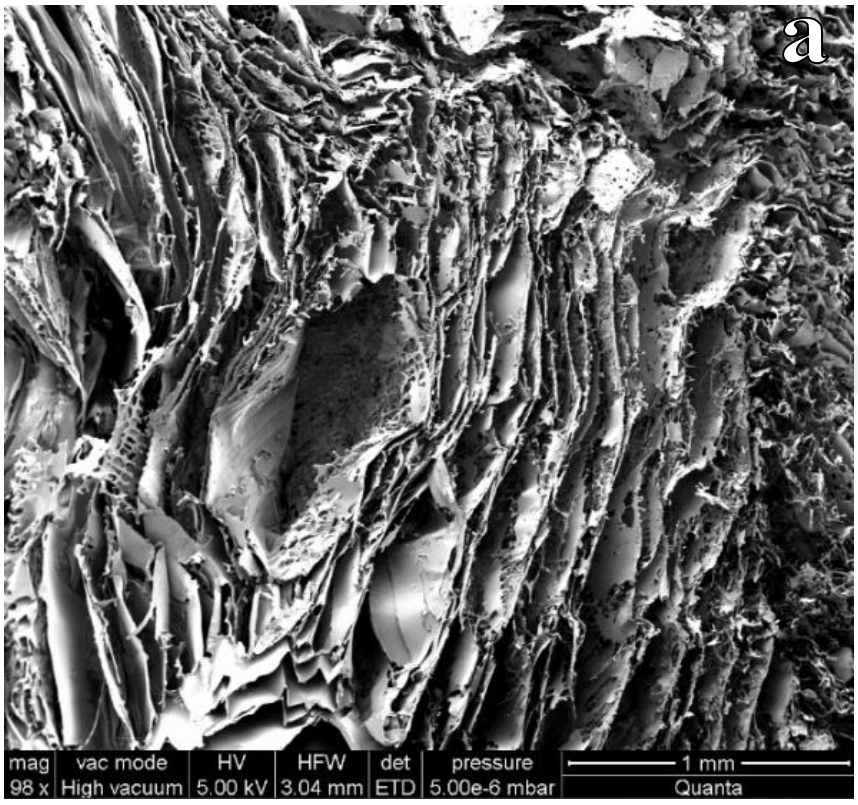

Figure 3.1: SEM images of F4-G0 (a), F3-G1 (b), F2-G2 (c), F1-G3 (d) and F0-G4 (e) samples.

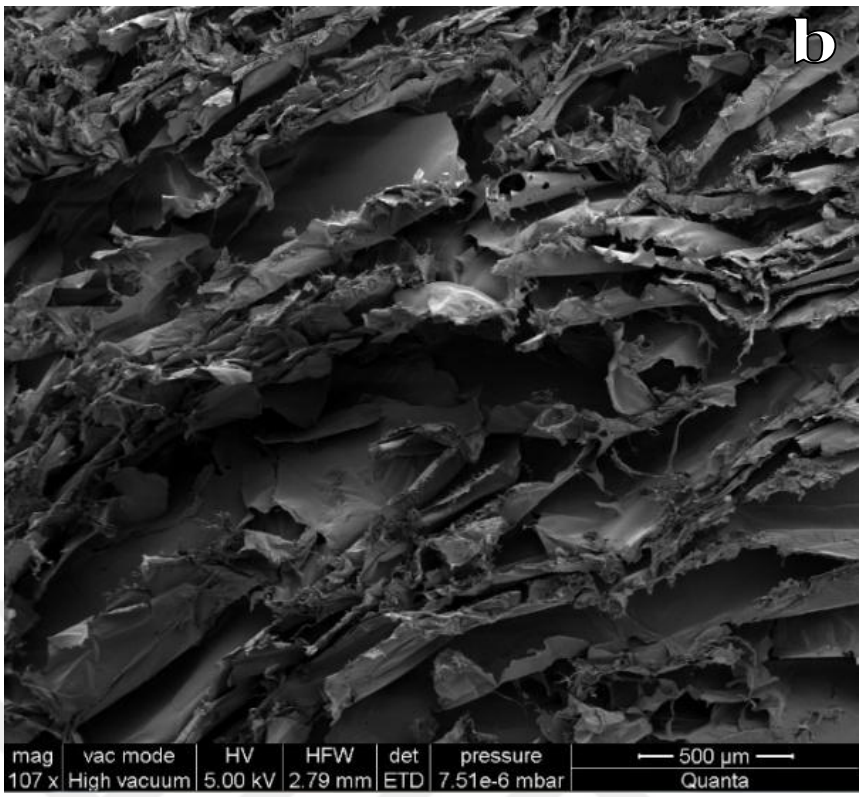

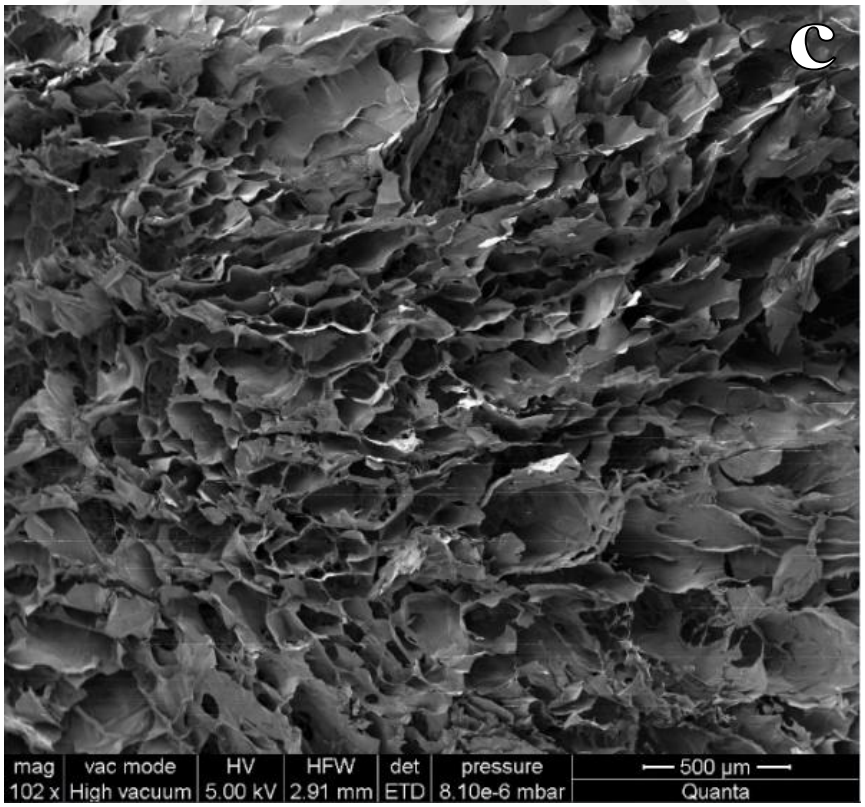

Figure 3.1 (continued): SEM images of F4-G0 (a), F3-G1 (b), F2-G2 (c), F1-G3 (d) and F0-G4 (e) samples.

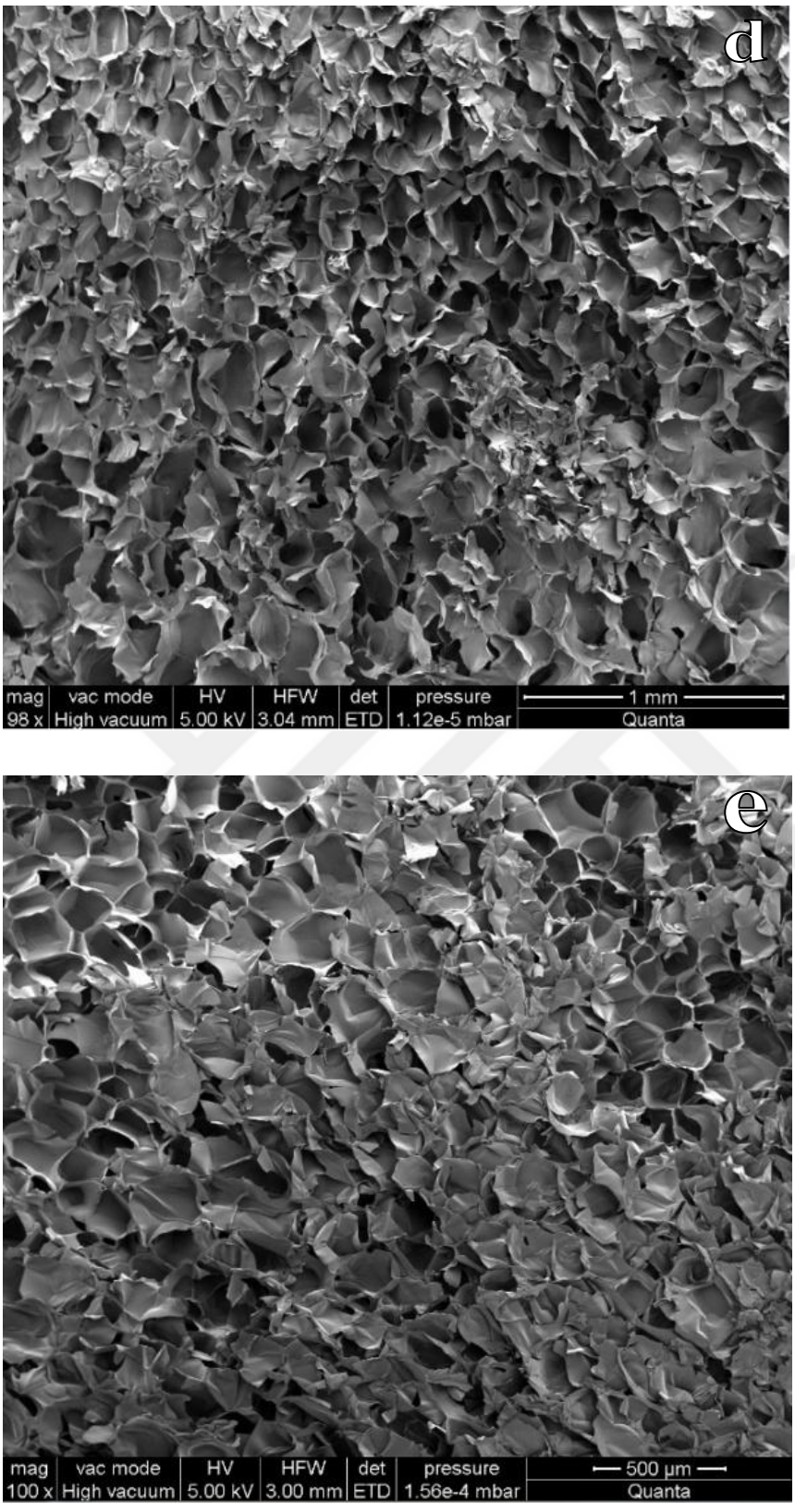

Figure 3.1 (continued): SEM images of F4-G0 (a), F3-G1 (b), F2-G2 (c), F1-G3 (d) and F0-G4 (e) samples.

3.1.2 Effect of methanol treatment on chemical structures of scaffolds

Methanol was reported to produce highly-stable beta-sheet protein secondary structure [76]. Thus, the effect of methanol treatment on the secondary structure of silk fibroin was investigated by comparing FTIR spectra of F3-G1, F2-G2 and F1-G3 samples with and without methanol treatment.

The secondary structure of silk fibroin is indicated by the amide groups of the silk proteins, and the positions of amide bands from FTIR spectra are used to determine random coil and β-sheet conformation of silk fibroin [77, 78].

Amide I, amide II and amide III bands, which are characteristics bands of peptide groups, were reported to appear at 1630 cm^{-1}, 1530 cm^{-1} and 1260 cm^{-1} for crystalline β-sheet structure, respectively. The bands at 1660 cm^{-1}, 1540 cm^{-1} and 1230 cm^{-1} that determine the amide I, amide II and amide III bands, respectively, are specific to the random coil form or silk I [79].

The F3-G1 scaffolds that were treated with methanol showed absorption bands at 1623 cm^{-1} (amide I), 1515 cm^{-1} (amide II) and 1233 cm^{-1} (amide III), whereas the F3-G1 scaffolds without methanol treatment provided absorption peaks at 1634 cm^{-1} (amide I), 1516 cm^{-1} (amide II) and 1235 cm^{-1} (amide III) (Figure 3.2). Therefore, it can be concluded that the absorption peaks of amide II and amide III bands remained almost unchanged and the absorption peak of amide I band was shifted to lower wave length in case of methanol treatment that may be resulted from β-sheet formation.

The F2-G2 scaffolds that were not treated with methanol showed absorption bands at 1636 cm^{-1} (amide I), 1527 cm^{-1} (amide II) and 1236 cm^{-1} (amide III), whereas the absorption peaks were obtained at 1625 cm^{-1} (amide I), 1516 cm^{-1} (amide II) and 1235 cm^{-1} (amide III) after the methanol treatment (Figure 3.3). Therefore, it can be concluded that the absorption peak of amide III band remained almost unchanged and the absorption peaks of amide I and amide II bonds was shifted to lower wave lengths in case of methanol treatment that may be resulted from β-sheet formation.

The F1-G3 scaffolds that were not treated with methanol showed absorption bands at 1631 cm^{-1} (amide I), 1532 cm^{-1} (amide II) and 1236 cm^{-1} (amide III). No significant change was obtained afther the methanol treatment and the absorption peaks were recorded as 1629 cm^{-1} (amide I), 1532 cm^{-1} (amide II) and 1235 cm^{-1} (amide III)

(Figure 3.4). Based on these data, it can be concluded that the F1-G3 composite scaffolds did not show any β-sheet formation.

Baimark *et. al.* [78] examined the effect of methanol treatment on random coil and β-sheet coformations of silk fibroin matrices. According to their results, the absorption bands of silk fibroin microparticles without methanol treatment were shown at 1655 cm^{-1} (amide I) and 1559 cm^{-1} (amide II), which were shifted to 1623 cm^{-1} (amide I) and 1530 cm^{-1} (amide II) in case of methanol treatment. These changes were attributed to predominant β-sheet conformation in methanol-treated silk fibroin microparticles.

In our study, however, methanol treatment did not cause significant changes in the chemical structure of F1-G3 scaffolds but there was a significant shift for F3-G1 and F2-G2 samples. In order to obtain β-sheet formation on the scaffolds, the duration of methanol treatment can be elongated. Additionally, the amount of methanol used can be reconsidered and utilised in higher amounts.

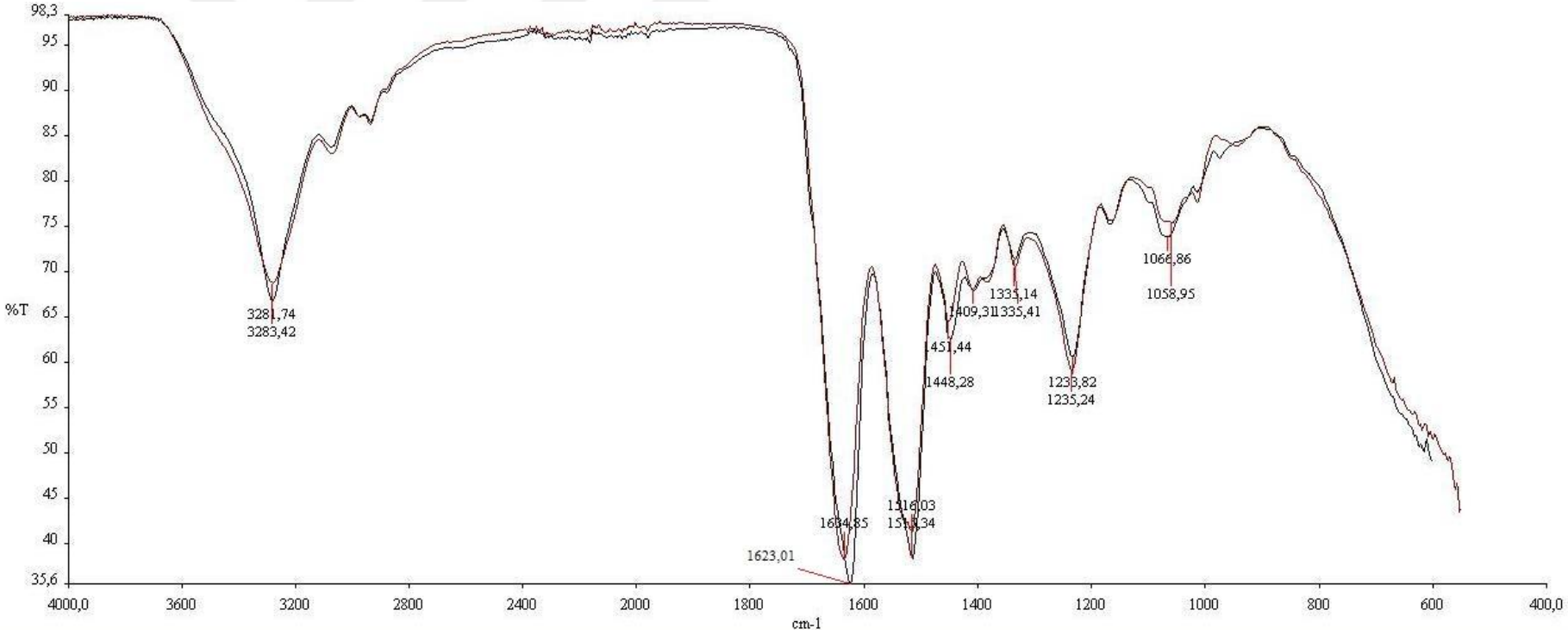

Figure 3.2: Comperative FTIR spectra of F3-G1 samples: The black line indicates the sample with methanol treatment, whereas the red line indicated the sample without methanol treatment.

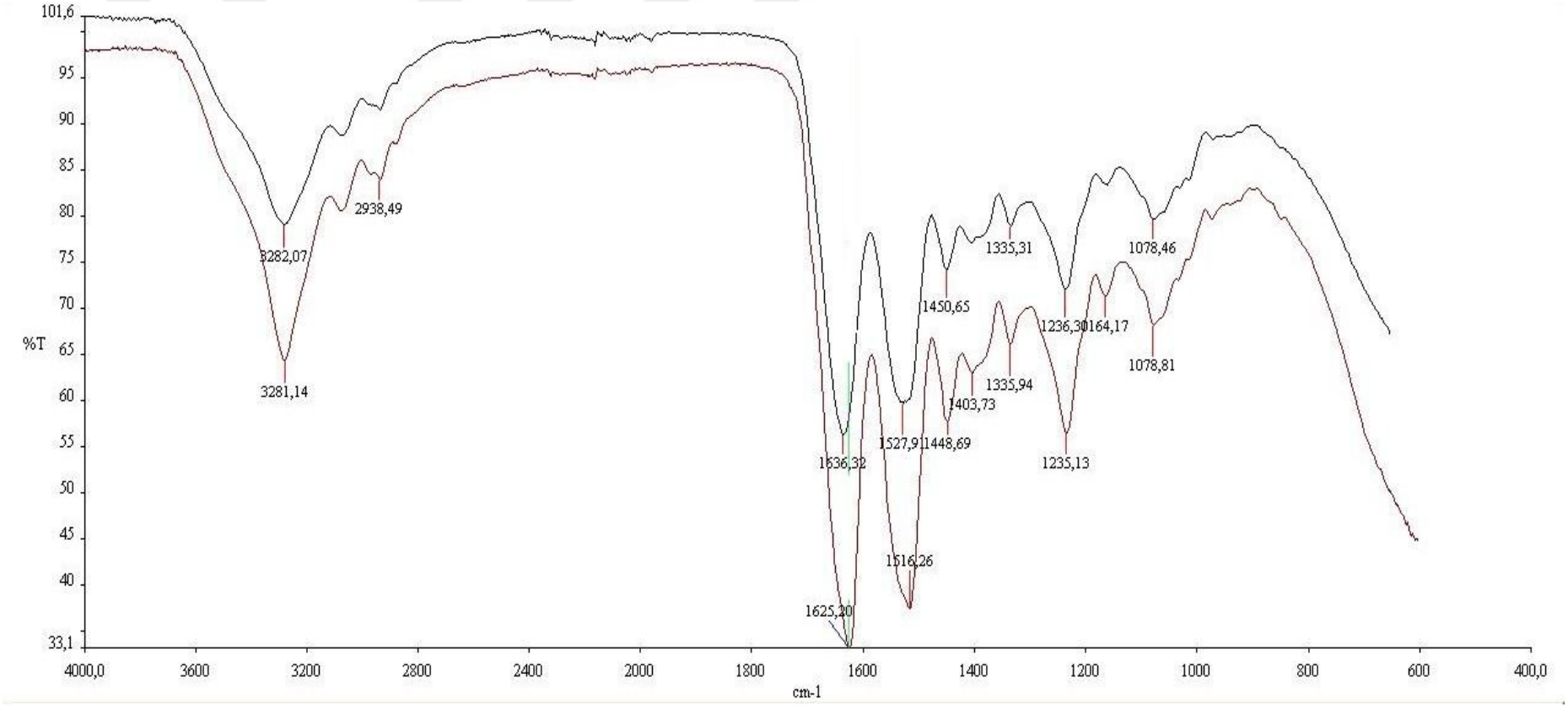

Figure 3.3: Comperative FTIR spectra of F2-G2 samples: The red line indicates the sample with methanol treatment, whereas the black line indicated the sample without methanol treatment.

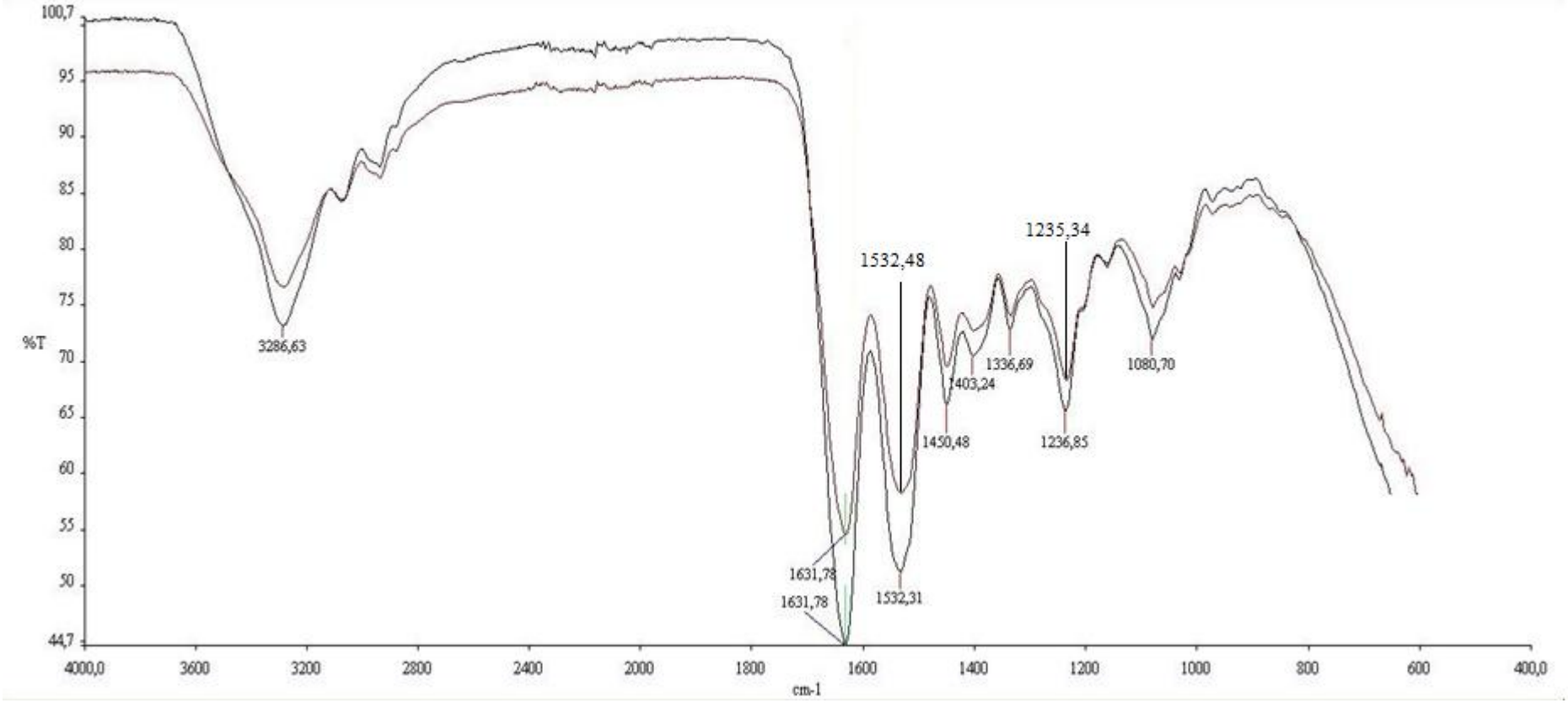

Figure 3.4: Comperative FTIR spectra of F1-G3 samples: The red line indicates the sample with methanol treatment, whereas the black line indicated the sample without methanol treatment.

3.2 Water-uptake and 3-day *in vitro* Biodegradation Analysis of Scaffolds

The results of 3-day *in vitro* biodegradation tests of F3-G1, F2-G2 and F1-G3 showed comparable differences (Table 3.1). Increasing gelatin ratio in blend solutions resulted in increased degradation rate at the same enzyme concentration. For samples treated with 0.05 U/mL Protease XIV, the average percentage of remaining weight after the 3rd day was 70% for F3-G1 scaffolds, where it was 65% and 18% for F2-G2 and F1-G3, respectively. The average remaining weight ratio of all samples showed a decreasing profile as the enzyme concentration was increased from 0.05 U/mL to 0.2 U/mL. Thus, F3-G1 with the lowest gelatin ratio showed less degradation after the 3th day of the tests. As a result, the enzyme concentration of 0.05 U/mL was selected for the 4-week *in vitro* biodegradation test since higher concentrations caused rapid and undesired degradation profile when a three-day period was taken into consideration.

Table 3.1: Results of water-uptake and 3-day *in vitro* biodegradation tests.

Scaffold Type	**Water-uptake (%)**	**Remaining weight after biodegradation (%)**		
		Treatment with 0.05 U/mL enzyme solution	**Treatment with 0.1 U/mL enzyme solution**	**Treatment with 0.2 U/mL enzyme solution**
F3-G1 (1)	873	74	63	42
F3-G1 (2)	648	66	63	77
F3-G1 (3)	869	71	68	68
Average	**797±105**	**70±3.3**	**65±2.4**	**62±14.8**
Control	-		**89**	
F2-G2 (1)	1386	64	65	37
F2-G2 (2)	1286	66	60	54
F2-G2 (3)	1141	64	64	36
Average	**1271±100**	**65±0.9**	**63±2.2**	**42±8.3**
Control	-		**75**	
F1-G3 (1)	871	21	2	5
F1-G3 (2)	1199	13	11	4
F1-G3 (3)	1090	19	27	2
Average	**1053±136**	**18±3.4**	**13±10.3**	**4±1.2**
Control	-		**23**	

The effect of blending ratio was studied by several scientists. However, there was no article found in the literature that compared the effect of different enzyme concentrations on *in vitro* biodegradation profiles of silk fibroin-gelatin composite scaffolds. For this purpose, Jetbumpenkul *et. al.* immersed different samples in 1 U/mL collagenase enzyme, incubated them under the conditions applied in this study, and observed that the degradation rate rapidly increased as the gelatin ratio in silk fibroin-composite scaffolds was increased. After 72 hours, the remaining weight percentages of silk fibroin, silk fibroin-gelatin scaffolds with equal polymer ratio, and gelatin scaffolds were around 95%, 35% and 0%, respectively. 70% and 5% of samples containing 80% silk fibroin and 20% gelatin, and 20% silk fibroin and 80% gelatin, respectively, remained at the end of the 72-hour period [7]. Although the type and concentration of enzyme solution and degradation rates of samples from the given reference study were different than those from this study, both could show that increasing gelatin concentration in silk fibroin-gelatin composite scaffolds led to an accelerated biodegradation.

The water-uptake properties of F3-G1, F2-G2 and F1-G3 samples displayed a different profile. The average water-uptake ratio of F3-G1 samples was approximately 797%, whereas 1271% and 1053% water-uptake ratios were observed for F2-G2 and F1-G3 samples, respectively. Among other two types of scaffolds, F2-G2 samples with equal silk fibroin and gelatin content had the highest water-uptake capacity at the end of a 1-day water-uptake period (Table 3.1).

Lerdchai *et. al*. also studied on silk fibroin-gelatin composite scaffolds immersed in PBS with pH 7.4 at 37 ^{o}C for 24 hours. Their results showed that the percentage of samples with equal silk fibroin and gelatin contents was 710%, whereas the highest percentage was observed for samples consisting of 15% silk fibroin and 85% gelatin polymers. The overall absorprtion percentages were around 706-732%, and there was no significant differences between all groups [75]. Unfortunately, all other publications contained different methods and polymers for water-uptake tests that disabled a reasonable comparison and conclusion for the effect of type and ratio of polymers on absorption pattern of silk fibroin-gelatin scaffolds.

Based on the results obtained from 3-day *in vitro* biodegradation test, the enzyme concentration of 0.05 U/mL and scaffold samples of F3-G1 and F2-G2 were chosen for further evaluation in the main biodegradation and biominerlisation tests.

3.3 *in vitro* Biodegradation Analysis of Scaffolds

3.3.1 Weight loss during the biodegradation analysis

The results of *in vitro* biodegradation tests for F3-G1 and F2-G2 samples showed comparable differences between each other after the pre-determined time periods of one week, two weeks, three weeks and four weeks.

For F3-G1 samples, the remaining weight ratio of samples showed a decreasing degradation profile throughout the whole process. Only exception for the 4-week period was the results obtained after the 3rd week due to unexpected degradation ratio for both one of the three degradation samples tested and the control sample. At the end of the test, the average percentage of remaining sample weight was 50%, whereas 69% of the control sample remained undegraded (Table 3.2). On the other hand, the biodegradation profile of F2-G2 samples showed a more steady degradation profile compared to that of F3-G1 samples. Degradation rate, however, seemed to decrease after the first week. At the end of the test period, the average percentage of remaining sample weight was 42%, whereas this value was 73% for the control sample (Table 3.2). In comparison with those of F3-G1, the F2-G2 samples showed a more rapid degradation rate during the first week of the test. The average remaining weight percentage at the end of the 1st week was 81% and 60% for F3-G1 and F2-G2 samples, respectively. At the end of the 2nd week, samples from both scaffold groups exhibited almost the same degradation rate (44% for F3-G1 samples and 42% for F2-G2 samples). A comparative analysis of biodegradation profile observed in both groups was given in Figure 3.5.

Table 3.2: Results of *in vitro* biodegradation tests for a) F3-G1 samples and b) F2-G2 samples.

	1st week		2nd week		3rd week		4th week	
	Remaining Weight[a] (%)	**Remaining Weight[b] (%)**	**Remaining Weight[a] (%)**	**Remaining Weight[b] (%)**	**Remaining Weight[a] (%)**	**Remaining Weight[b] (%)**	**Remaining Weight[a] (%)**	**Remaining Weight[b] (%)**
1st sample	88	61	71	62	50	63	48	43
2nd sample	83	60	50	57	44	48	53	37
3rd sample	71	60	48	54	26	35	49	45
Average (%)	**81±7.1**	**60±0.5**	**56±10.4**	**58±3.3**	**40±10.2**	**49±11.4**	**50±2.2**	**42±3.4**
Control sample	**99**	**76**	**94**	**76**	**56**	**74**	**69**	**73**

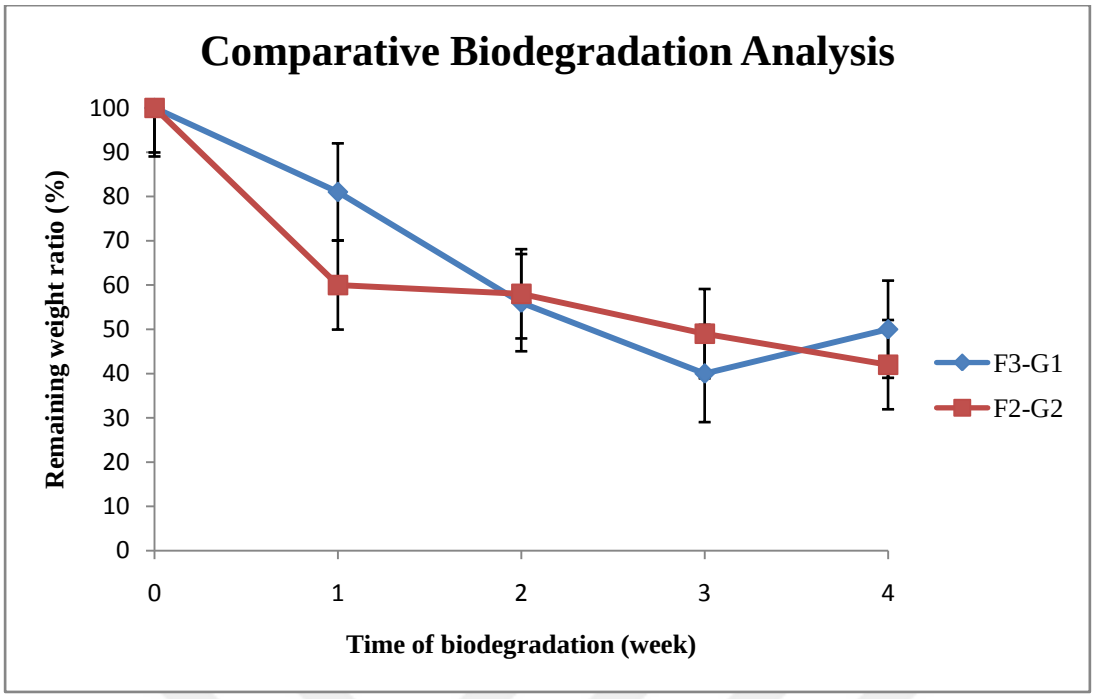

Figure 3.5: Comparative biodegradation results of F3-G1 and F2-G2 samples.

As previously stated, several researchers examined the impact of polymer ratios in silk fibroin-gelatin composite scaffolds on *in vitro* biodegradation behaviour. For example, Lerdchai *et. al.* performed a 28-day biodegradation test for silk fibroin-gelatin constructs with various polymer blending ratios including 100/0, 80/20, 50/50, 20/80 and 0/100 of silk fibroin and gelatin, respectively. They incubated silk fibroin-gelatin sponges in 1U/mL collagenase solution (pH 7.4) containing 0.01% (w/v) sodium azide at 37 ^{o}C. According to their results, the degradation profiles of all sponges were similar during the first 8 days. However, the remaining weight of gelatin sponges at the end of the test was lower than those of other sponges, indicating that gelatin had the highest biodegradation rate (>30%). On the other hand, the lowest and highest degradation rates of silk fibroin-gelatin sponges were 10% and 20%, respectively [75].

The difference observed in biodegradation profiles of samples comprising the same polymers in different ratios may be a result of structural changes that emerged due to the interactions between silk fibroin and gelatin polymers. The results indicated that the degradation rate and profile of silk fibroin-gelatin composite scaffolds can be controlled by adjusting the polymer blending ratios. Due to limited number of studies that conducted the biodegradation rate in the same way with this study, additional comprehensive assessments could not be done. Another reason for the difference in

biodegradation profiles may be the restricted protease enzyme accessibility within the scaffolds because of the methanol treatment and glutaraldehyde presence in the samples.

3.3.2 Morphology change during the biodegradation analysis

SEM images for F3-G1 and F2-G2 samples were taken after the *in vitro* biodegradation assays. The 4-week biodegradation test increased the porous properties of some of the F3-G1 and F2-G2 samples (Figure 3.6, Figure 3.7) and led to more porous scaffold surfaces. According to the SEM images, the F3-G1 samples of the 3rd and the 4th weeks and the F2-G2 sample of the 2nd week did not show any significant change in terms of porous morphology.

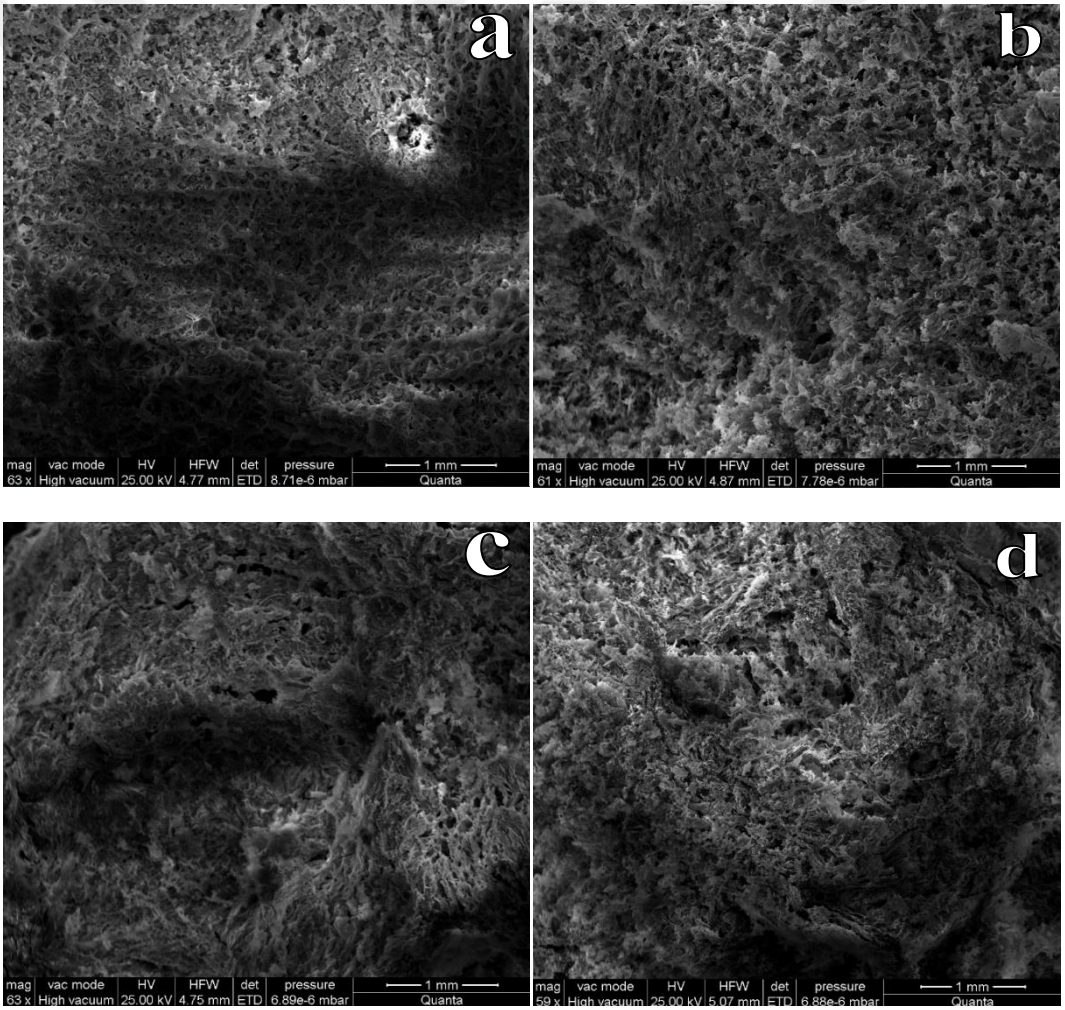

Figure 3.6: SEM images of F3-G1 samples after the 1st (a), 2nd (b), 3rd (c) and 4th week of *in vitro* biodegradation test.

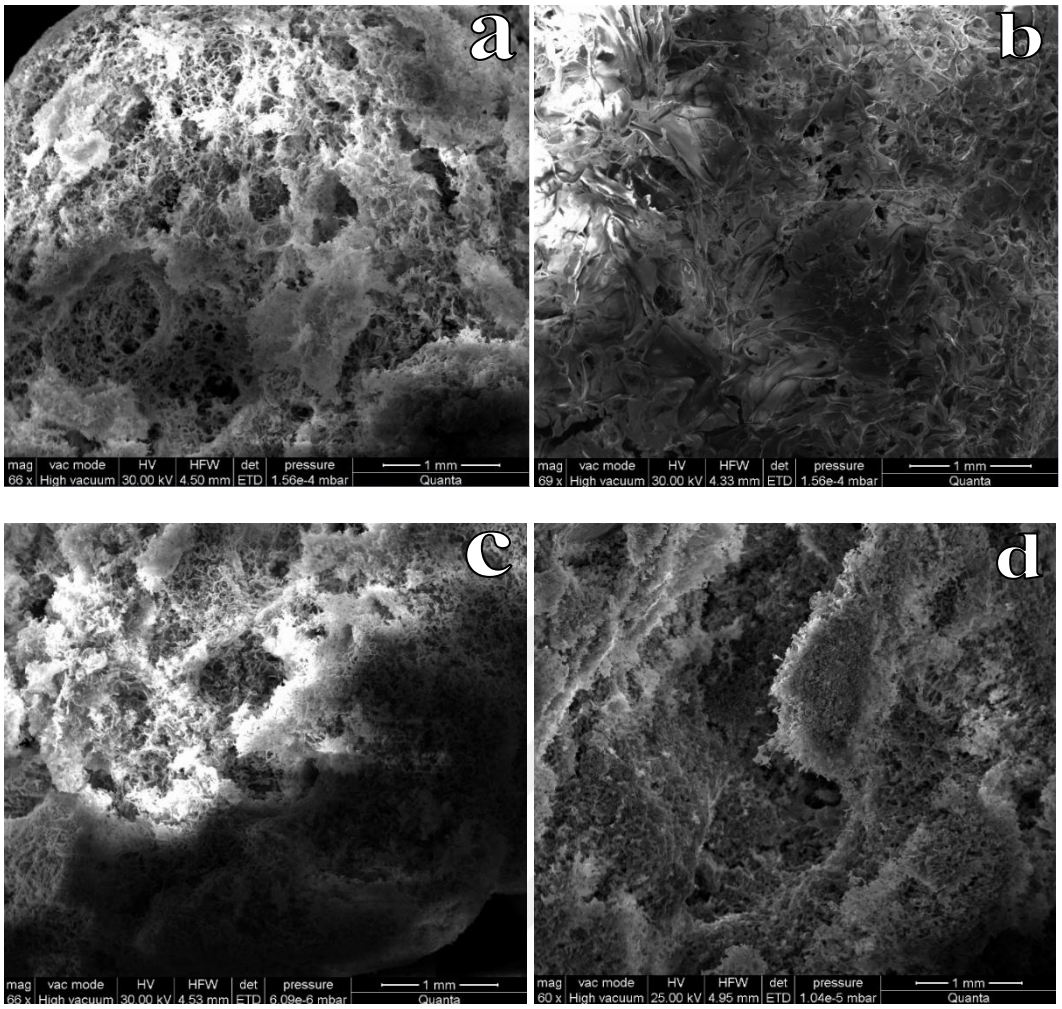

Figure 3.7: SEM images of F2-G2 samples after the 1st (a), 2nd (b), 3rd (c) and 4th week of *in vitro* biodegradation test.

3.4 *in vitro* Biomineralisation Analysis of Scaffolds

in vitro biomineralisation test that was described in Section 2.2.7 was performed in order to induce hydroxyapatite crystal formation on scaffold surfaces. The presence of hydroxyapatite crystals were determined by scanning electron microscopy and fourier transform infrared spectroscopy. The SEM images were taken at approximately 230x magnification, whereas the FTIR spectra of scaffolds with and without mSBF treatment were compared.

3.4.1 Scanning electron microscopy analysis

The SEM images of F3-G1 scaffolds that were immersed in either 1x and or 3x mSBF solutions were given in Figure 3.8 and Figure 3.9, respectively. However, hydroxyapatite formation could only be seen in F3-G1 scaffolds at the end of the 1st day of the test with 1x mSBF that was indicated with red circles in Figure 3.8a. This

may be resulted from damaged overall shape of the samples that prevented distinct sample imaging or the magnification level of SEM images.

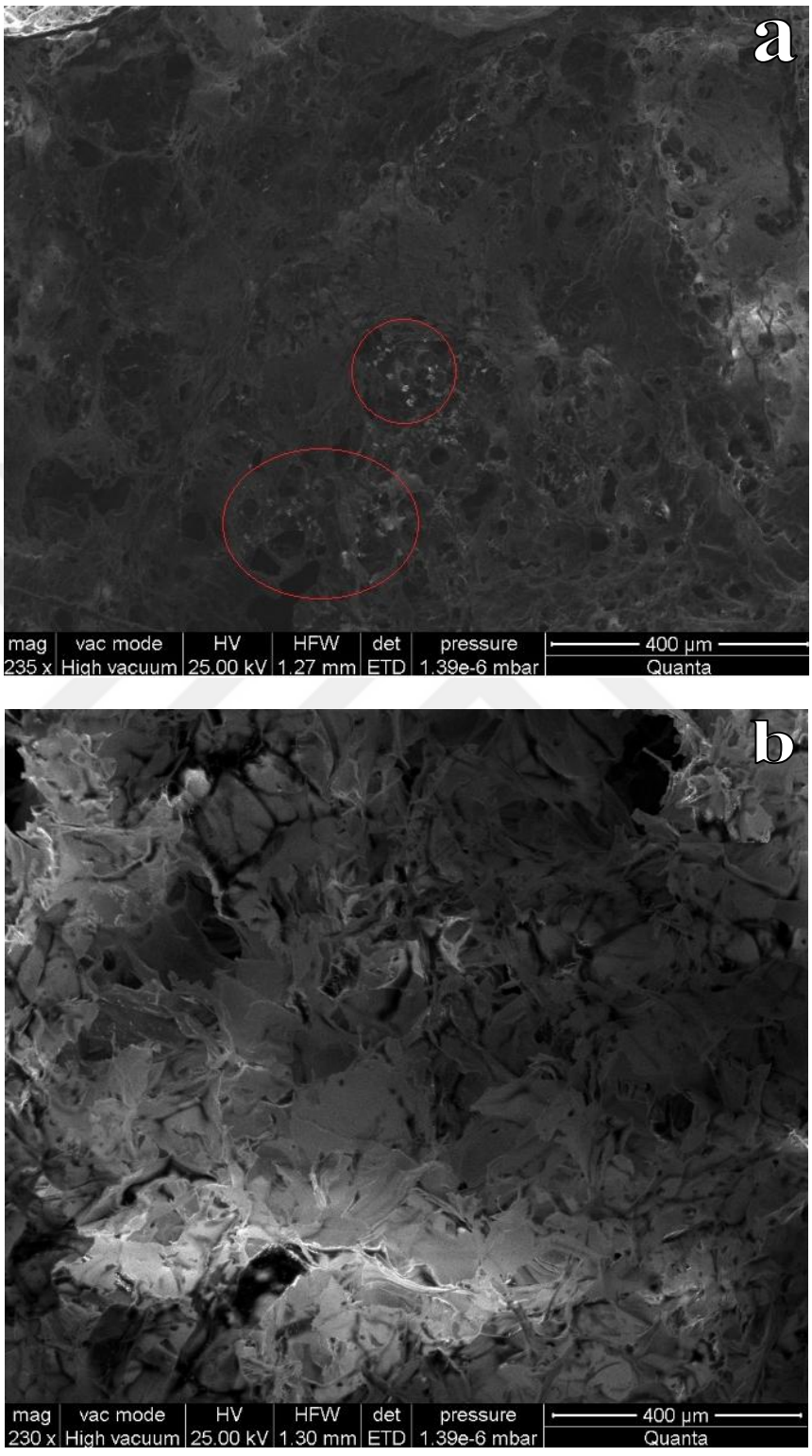

Figure 3.8: SEM images of F3-G1 samples after the 1st (a), 4th (b) and 7th (c) days of *in vitro* biomineralisation test with 1x mSBF.

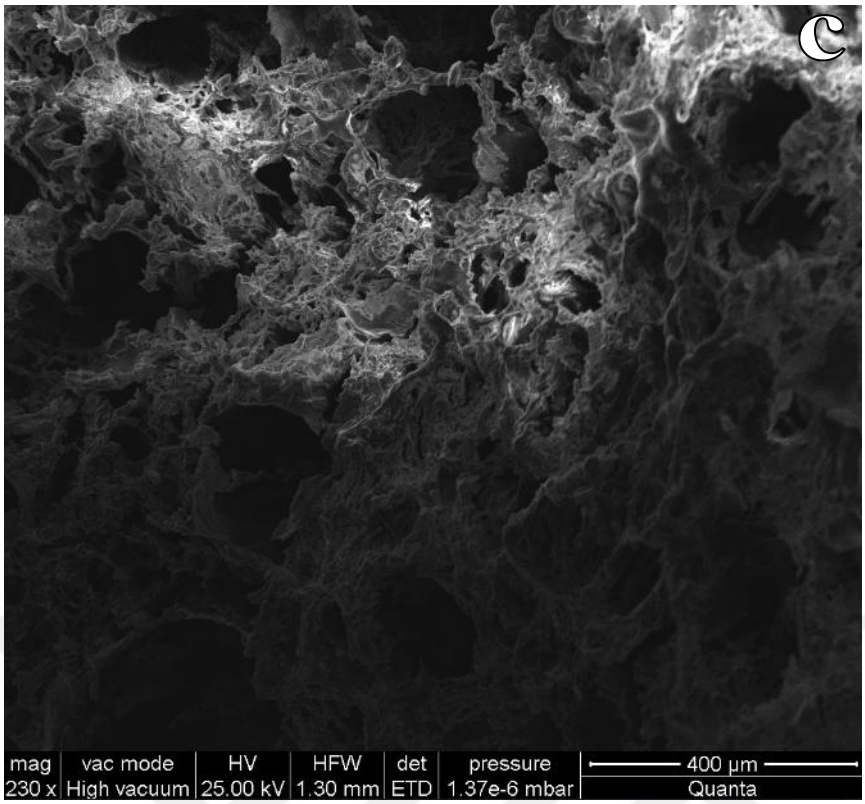

Figure 3.8 (continued): SEM images of F3-G1 samples after the 1st (a), 4th (b) and 7th (c) days of *in vitro* biomineralisation test with 1x mSBF.

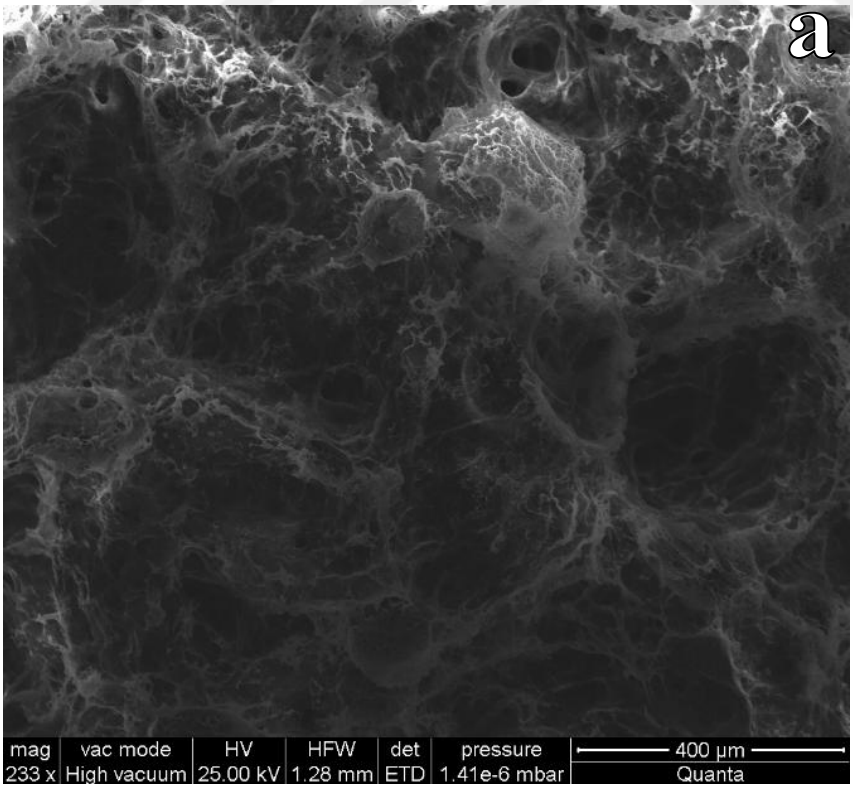

Figure 3.9: SEM images of F3-G1 samples after the 1st (a), 4th (b) and 7th (c) days of *in vitro* biomineralisation test with 3x mSBF.

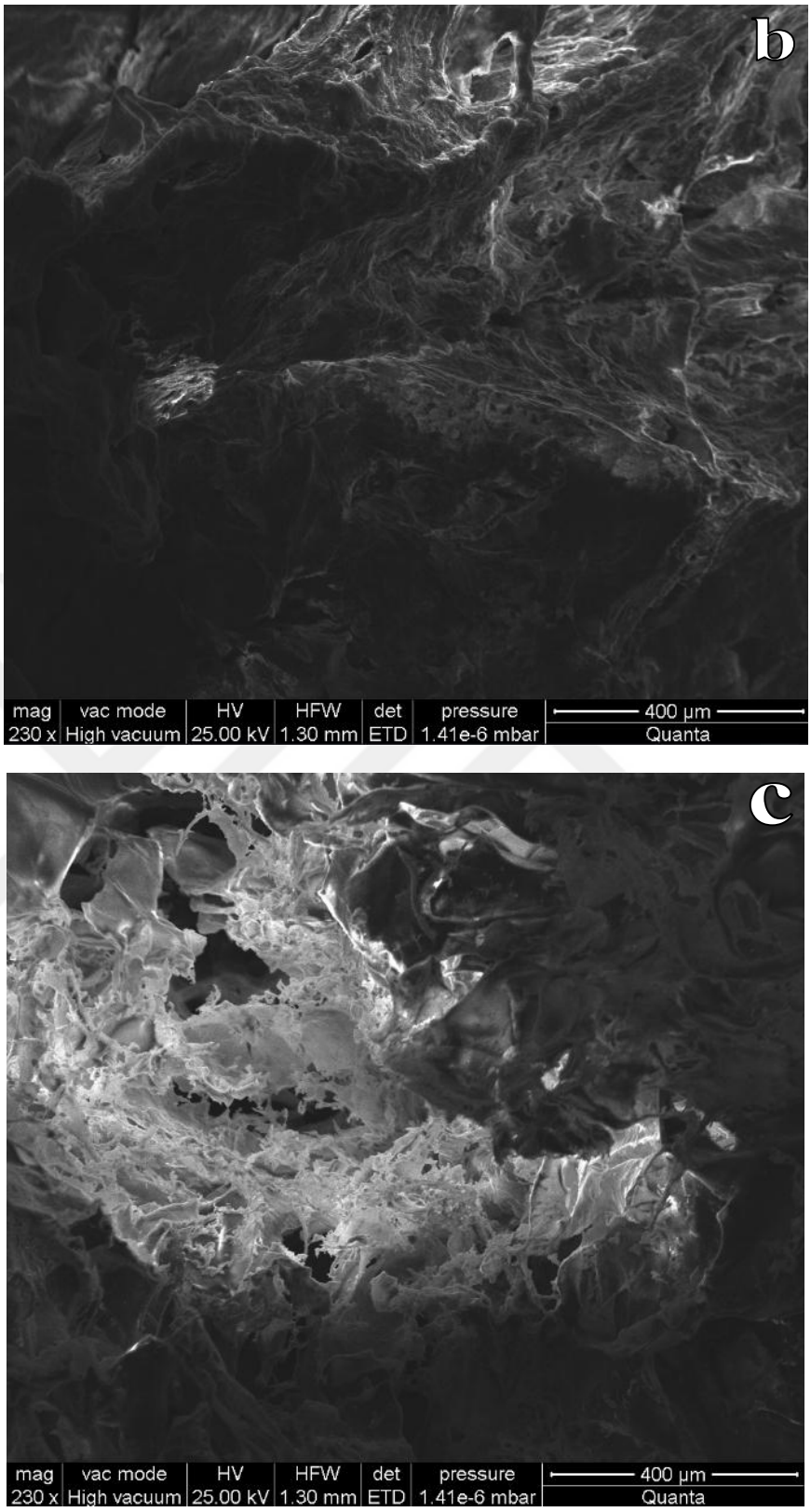

Figure 3.9 (continued): SEM images of F3-G1 samples after the 1st (a), 4th (b) and 7th (c) days of *in vitro* biomineralisation test with 3x mSBF.

The SEM images of F2-G2 scaffolds that were immersed either in 1x and or in 3x mSBF solutions were given in Figure 3.10 and Figure 3.11, respectively and hydroxyapatite crystals were indicated with red circles in Figure 3.10a, 3.10c, 3.11a and 3.11c, which corresponds to 1st and 7th weeks for 1X and 3X mSBF samples. However, hydroxyapatite formation could not be observed on the samples collected at day of 4. This may be resulted from damaged overall shape of the samples that prevented distinct sample imaging. As a result, FTIR spectra were compared and assessed to detect any possible hydroxyapatite formation for all samples.

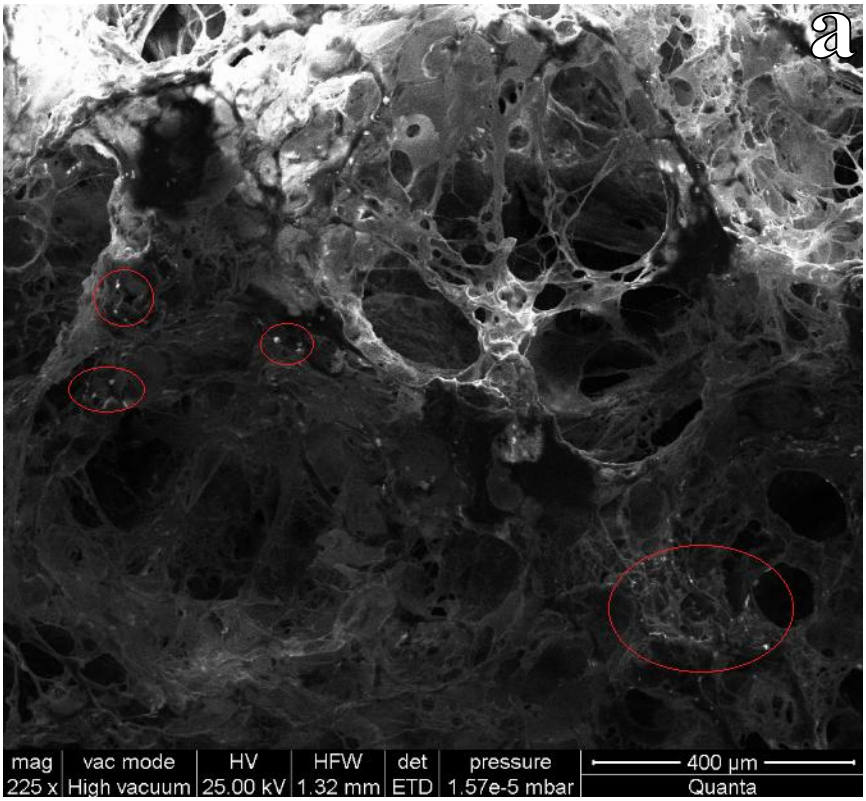

Figure 3.10: SEM images of F2-G2 samples after the 1st (a), 4th (b) and 7th (c) days of *in vitro* biomineralisation test with 1x mSBF.

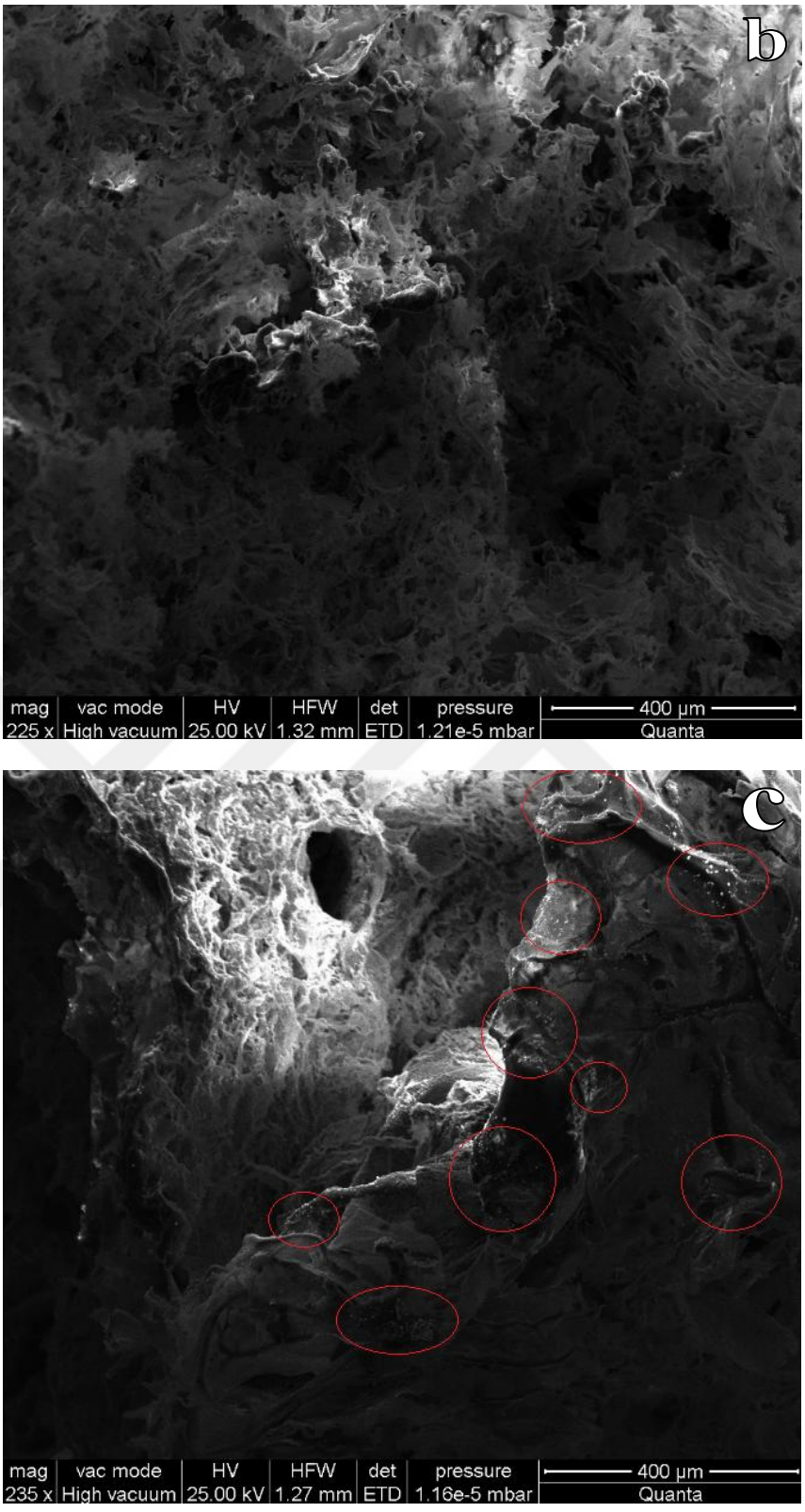

Figure 3.10 (continued): SEM images of F2-G2 samples after the 1st (a), 4th (b) and 7th (c) days of *in vitro* biomineralisation test with 1x mSBF.

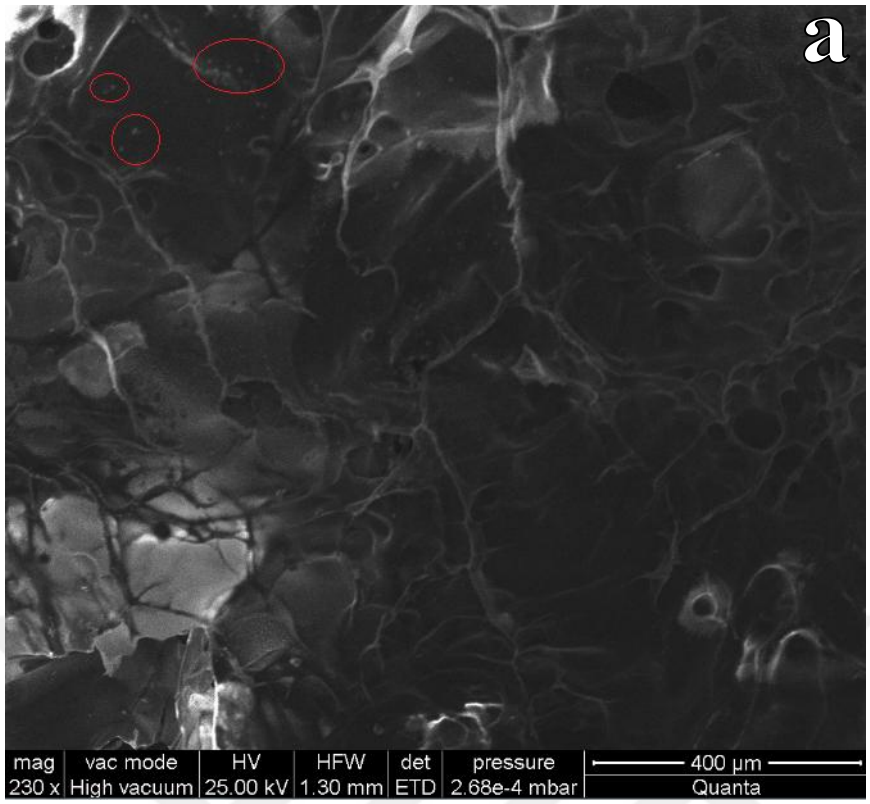

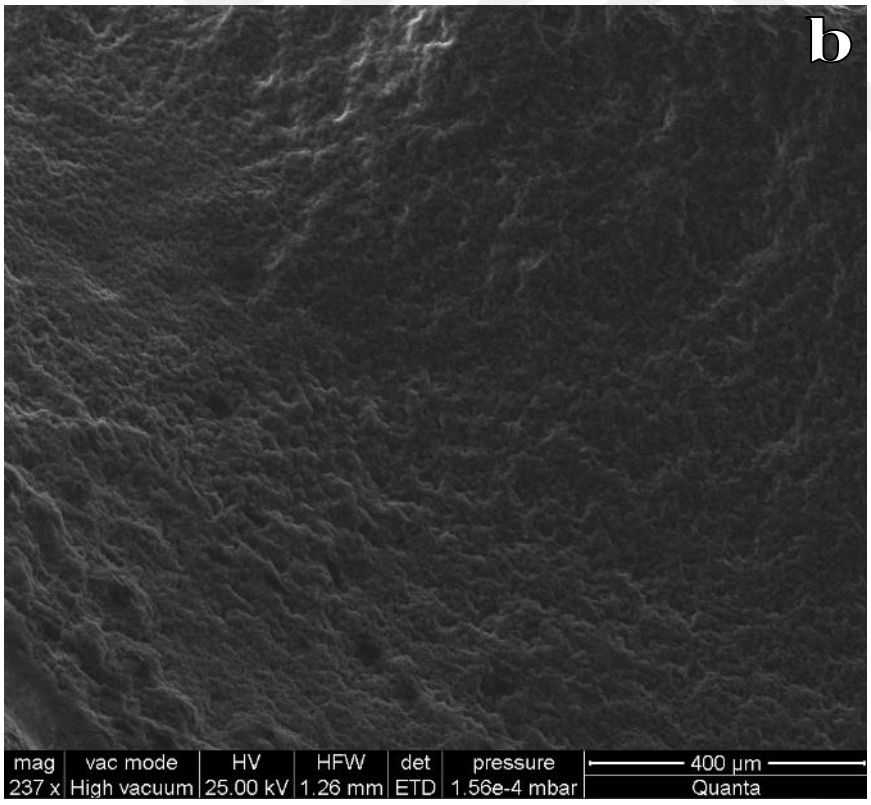

Figure 3.11: SEM images of F2-G2 samples after the 1st (a), 4th (b) and 7th (c) days of *in vitro* biomineralisation test with 3x mSBF.

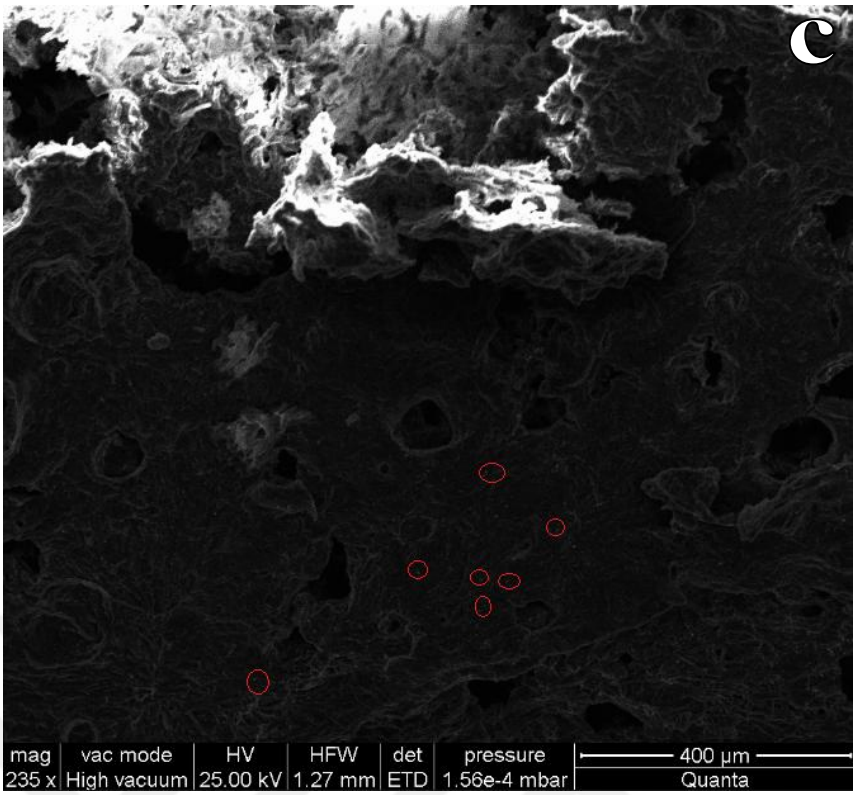

Figure 3.11 (continued): SEM images of F2-G2 samples after the 1st (a), 4th (b) and 7th (c) days of *in vitro* biomineralisation test with 3x mSBF.

3.4.2 Fourier transform infrared spectroscopy analysis

Berzina-Cimdina *et. al.* reported that the most characteristic chemical groups in FTIR spectra of synthesised hydroxyapatites are PO_4^{3-}, OH^-, CO_3^{2-}, and HPO_4^{2-}, which were reported by many researchers to form absorption peaks at different wave lengths (Table 3.3) [80].

Table 3.3: FTIR absorption bands of synthesised hydroxyapatite chemical groups.

Chemical group	Absorption bands (cm^{-1})	Description
PO_4^{3-}	460; 560-600; 960; 1020-1120; 1040; 1000-1100	Intensive absorption bands at 560, 600 and 1000-1100 cm^{-1}
OH^-	3500; 630 and 3540; 3570 and 3420; 1650	OH^- ions that prove presence of hydroxyapatites.
CO_3^{2-}	873; 1450; 1640; 1650; 870 and 880; 1460 and 1530	Weak peaks between 870 and 880 cm^{-1}; more intensive peaks between 1460 and 1530 cm^{-1}
HPO_4^{2-}	875; 880	HPO_4^{2-} characterises calcium-deficient hydroxapatite crystals.

The F3-G1 scaffolds that were immersed in 1x mSBF started to show absorption peaks at approximately 1170 cm^{-1} after the 1st day. In addition, a new absorption peak at approximately 1040 cm^{-1} was emerged in all samples that were treated with

1x mSBF. Both of these absorption peaks were most intensively seen at the end of the 7^{th} day (Figure 3.12).

For F3-G1 scaffold that was immersed in 3x mSBF, a similar pattern was observed. There was a new absorption peak at 1170 and 1040 cm^{-1} beginning from the 1^{st} day. Both of these absorption peaks were most intensively seen at the end of the 4^{th} and 7^{th} days (Figure 3.13).

Based on the information and data given above, for all of the F3-G1 samples, the absorption peaks at approximately 1170 cm^{-1} as well as the ones at 1040 cm^{-1} could be attributed to the presence of the PO_4^{3-} groups on the surface, hence biomineralisation.

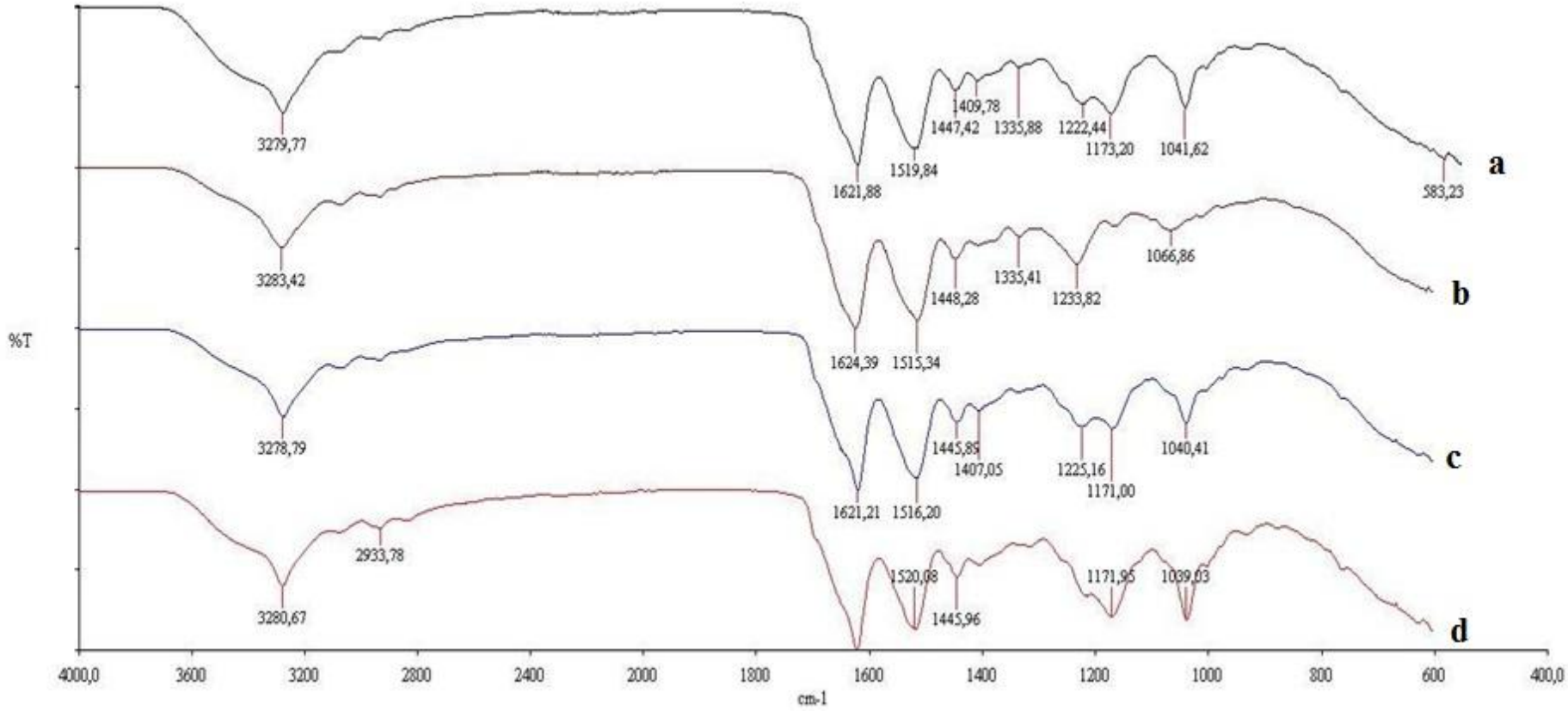

Figure 3.12: Comparative FTIR spectra of F3-G1 samples without (b) and after the 1st (c), 4th (d) and 7th (a) days in biomineralisation test with 1x mSBF.

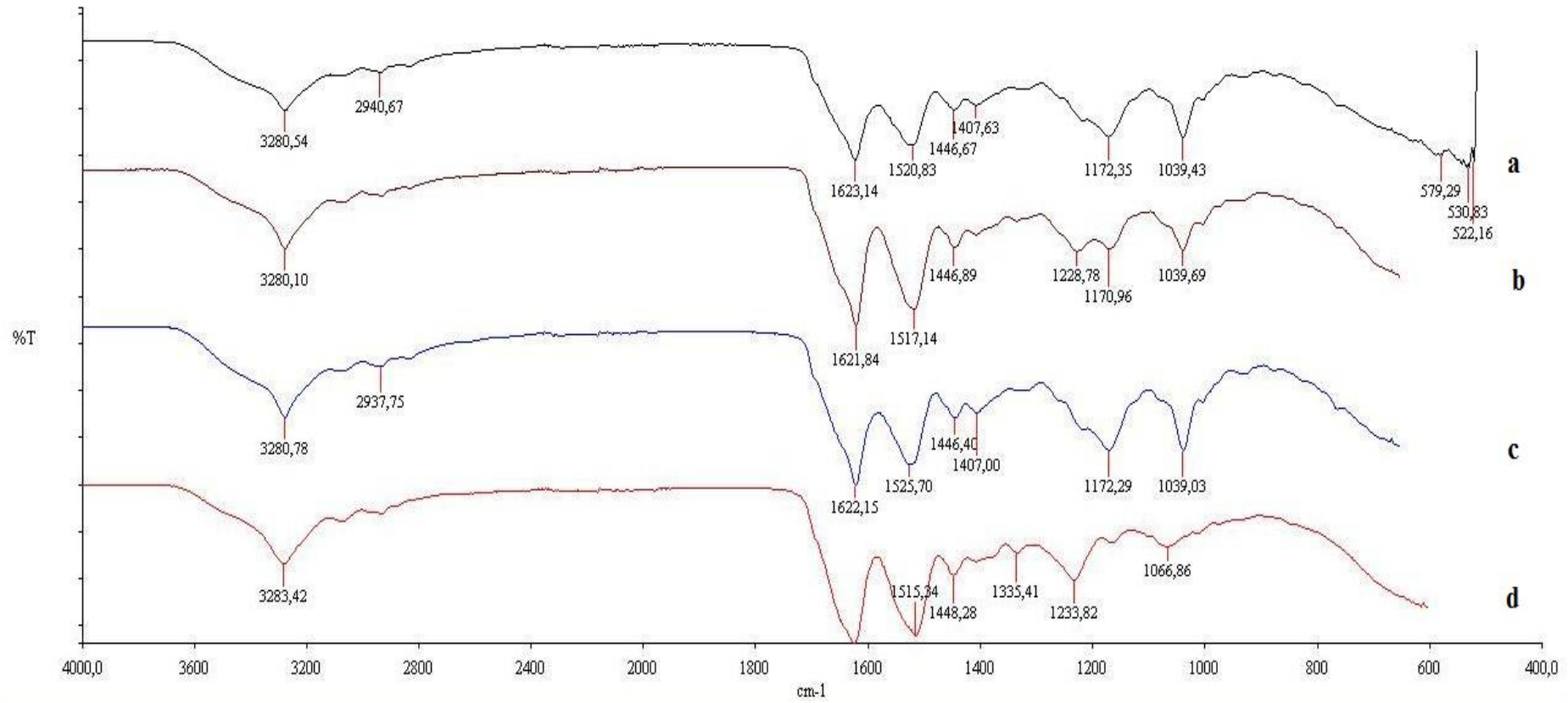

Figure 3.13: Comparative FTIR spectra of F3-G1 samples without (d) and after the 1st (b), 4th (c) and 7th (a) days in biomineralisation test with 3x mSBF.

As previously explained for the FTIR spectra of F3-G1 scaffolds, the most characteristic chemical groups in FTIR spectra of synthesised hydroxyapatites are PO_4^{3-}, OH^-, CO_3^{2-}, and HPO_4^{2-}, and the wave lengths at which they form absorption peaks were already given in Table 3.3.

The F2-G2 scaffolds that were immersed in 1x mSBF showed weak absorption peaks at approximately 1040 cm^{-1} beginning from the 1st day. The sample that was collected at the of the 7th day showed an additional weak absorption peak at 1206 cm^{-1} and many weak absorption weaks between 1049 and 767 cm^{-1}, with the most intensive one at 879 cm^{-1}, which may be formed due to the presence of the CO_3^{2-} group (Figure 3.14).

The absorption peak at 1235 cm^{-1} of the untreated F2-G2 scaffold was shifted to 1232, 1221 and 1173 cm^{-1} for the 1st, 4th and 7th day samples, respectively, after it was immersed in 3x mSBF. Another absorption peak that was formed for the sample without mSBF-treatment at 1078 cm^{-1} was also shifted to 1037 cm^{-1} at the end of the 1st and 4th days and to 1039 cm^{-1} at the end of the 7th day. The absorption peaks at 1173 and 1039 cm^{-1} for the 7th day sample showed more intensive bands than their equivalent peaks that were seen in other samples (Figure 3.15).

According to the FTIR spectra and data of the F2-G2 scaffolds, the absorption peaks at 1040 and 1049 cm^{-1} for the samples that were treated with 1x mSBF may be resulted from the PO_4^{3-} groups. For the sample that were treated with 3x mSBF for the 7th day, the absorption peak at 1173 cm^{-1} may also be formed because of the presence of the PO_4^{3-} groups. The absorption bands at approximately 1037 cm^{-1} that were seen in samples immersed in 3x mSBF probably showed the formation of the PO_4^{3-} groups.

Composite scaffolds comprising different polymers and hydroxyapatite crystals were studied by several scientists. However, there was no article found in the literature that was focused on the hydroxyapatite formation on silk fibroin-gelatin composite scaffolds. Cholas *et. al.* incorporated hydroxyapatite microspheres into collagen scaffolds with interconnected porosity and showed phosphoric groups at 1025 and 1047 cm^{-1} and CO_3 bands at 1445, 1414 and 876 cm^{-1} according to the FTIR spectra of their samples [81]. In a recent study, Tsiourvas *et. al.* aimed to develop porous chitosan scaffolds with high nano-hydroxyapatite content and examined the FTIR

spectra of hydroxyapatite-chitosan scaffolds and showed absorption bands at 1090, 1044, 1019 and 962 cm^{-1} that were assigned to the phosphate groups [82]. In another study, Sharma *et. al.* fabricated a composite scaffold from chitosan, gelatin, alginate and nano-hydroxyapatite with the aim of producing a biomimetic construct for bone tissue engineering applications. In the FTIR spectra they obtained in their study, nano-hydroxyapatite molecules formed a peak at 1030, 604 and 563 cm^{-1} that were attributed to the PO_4^{3-} stretching and bending vibrations [83].

According to the all data from the study and information adapted from references, it can be concluded that *in vitro* biomineralisation tests of F3-G1 and F2-G2 scaffolds led to hydroxyapatite formation on scaffold surfaces to some extent that could not be easily observed by SEM, but some characteristic absorption peaks could be clearly detected in the FTIR spectra of the samples.

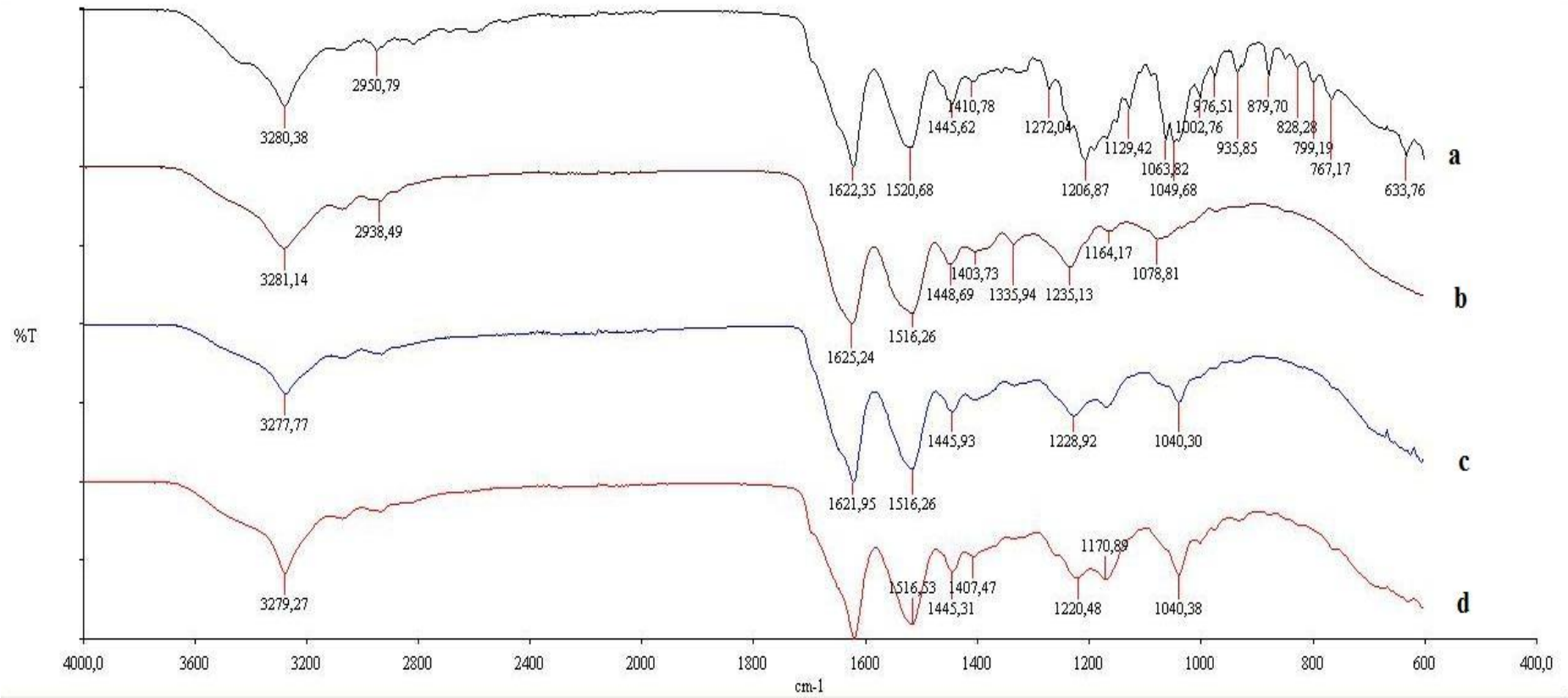

Figure 3.14: Comparative FTIR spectra of F2-G2 samples without (b) and after the 1st (c), 4th (d) and 7th (a) days in biomineralisation test with 1x mSBF.

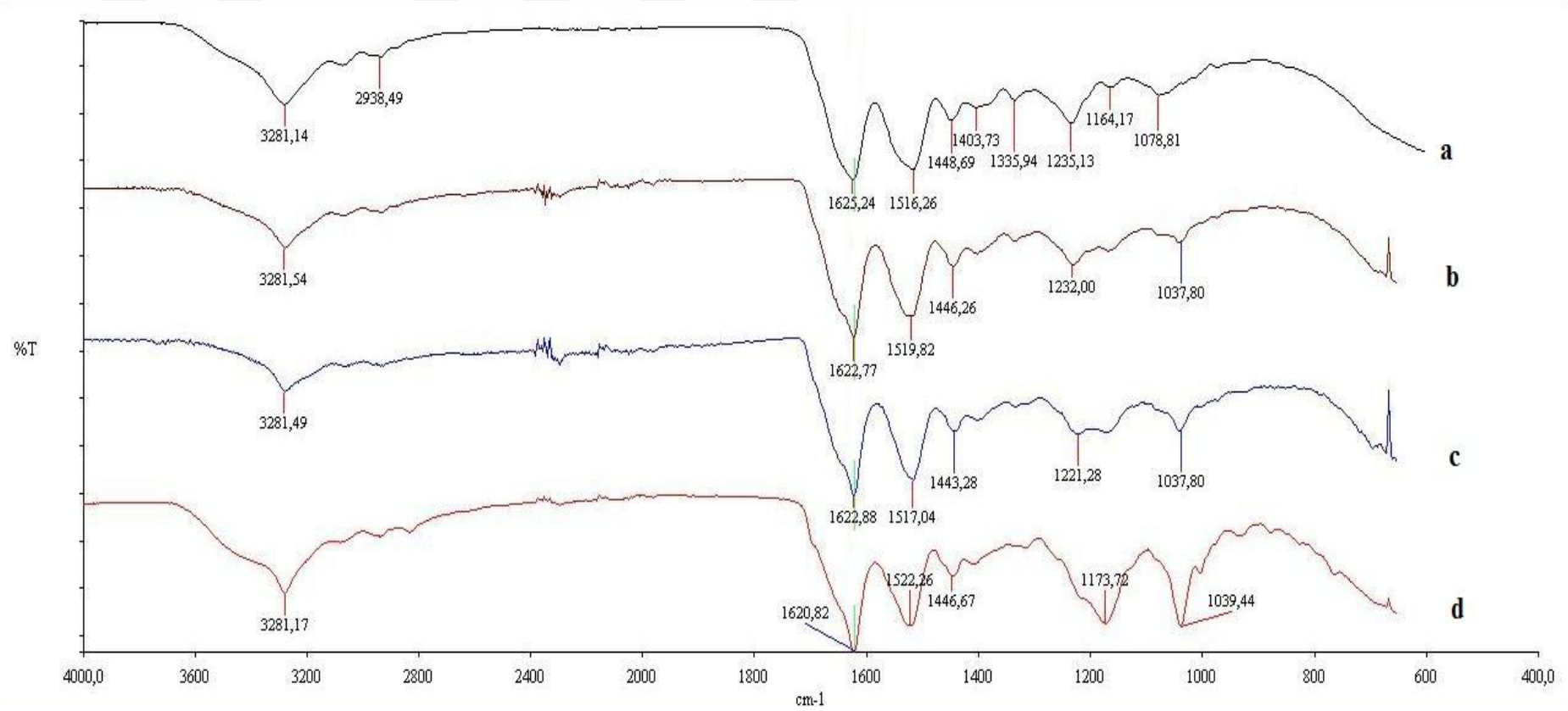

Figure 3.15: Comparative FTIR spectra of F2-G2 samples without (a) and after the 1st (b), 4th (c) and 7th (d) days in biomineralisation test with 3x mSBF.

4. CONCLUSIONS AND RECOMMENDATIONS

Chemical, biological, mechanical and structural properties of scaffolds and the type of the biomaterials that are used to fabricate these biomimetic constructs are essential factors for successful tissue engineering applications. The aim of this study was to fabricate biocompatible and biodegradable 3D scaffolds for bone tissue engineering applications with desired tissue-specific features. To do this, silk fibroin that was extracted from *Bombyx mori* silkworm cocoons and gelatin that was commercially purchased were used in different blending ratios as the natural components of the composite scaffolds. Glutaraldehyde and methanol were additionally incorporated to the blend solutions as chemical agents that led to cross-linked gelatin polymers and silk fibroin polymers with β-sheet structures, respectively. The composite scaffolds with 100/0, 75/25, 50/50, 25/75 and 0/100 blending ratios were named as F4-G0, F3-G1, F2-G2, F1-G3 and F0-G4, respectively, and their morphologies were examined by Scanning Electron Microscopy (SEM).

The SEM images showed that increased gelatin ratio in silk fibroin-gelatin composite scaffolds resulted in more porous scaffold structures. According to the FTIR spectra of these scaffolds, methanol treatment induced β-sheet formation in samples with higher fibroin content (F3-G1 and F2-G2).

Based on the data obtained from the 3-day and 28-day biodegradation studies, the average remaining weight percentage was lower for composite scaffolds with higher gelatin ratio at the end of both tests, indicating that increased gelatin ratio led to more erosion in the composite scaffolds. However, there was no direct correlation between gelatin ratio and water-uptake capacity of the scaffolds. On the other hand, biodegraded samples showed more porous structures to some extent when compared with their equivalents before the test.

Hydroxyapatite crystals were clearly observed in most of the samples with higher gelatin contents. However, the samples treated with mSBF of lower concentration exhibited more crystals than those treated with higher concentration mSBF.

Regardsless of the mSBF concentration used, the SEM images of the scaffolds with lower gelatin contents showed hydroxyapatite formation in only one sample. Some hydroxyapatite-specific absorption bands could be detected in the FTIR spectra of all samples.

In conclusion, the gelatin content directly affected the morphology and biodegradation profiles of silk fibroin-gelatin composite scaffolds, indicating that the porosity and biodegradation duration and course can be controlled by adjusting gelatin ratios in the samples. The number and intensity of the absorption bands that are specific to hydroxyapatite crystals were higher for the samples with high gelatin content. On the other hand, gelatin did not have a significant impact on the water-uptake capacity of the scaffolds.

For future prospects, the composite scaffolds that were produced in this study can be further studied and evaluated by peptide immobilisation and cell culture tests in order to investigate their potential for bone tissue engineering applications. Once these tests exhibit positive results, *in vivo* experiments can be performed by using animal models to show applicability of the whole system consisting of scaffold, seeded cells and biological molecules to human. The scaffold composition, polymer blending ratios, amount of chemical agents, parametres of lyophilisation, water-uptake, biodegradation and biomineralisation tests can be rearranged in order to assess and improve the outcomes of this study.

REFERENCES

[1] **Sionkowska, A. and Płanecka, A.** (2013). Preparation and characterization of silk fibroin/chitosan composite sponges for tissue engineering. *Journal of Molecular Liquids*, ***178***, 5-14.

[2] **Li, M., Minoura, N., Ogiso, M.** (2003). Enzymatic degradation behavior of porous silk fibroin sheets. *Biomaterials*, ***24***, 357-365.

[3] **Yang, Z., Xu, L. S., Yin, F., Shi, Y. Q., Han, Y., Zhang, L., Jin, H. F., Nie, Y. Z., Wang, J. B., Xing, H., Fan, D. M., Zhou, X. M.** 2012. *In vitro* and *in vivo* characterization of silk fibroin/gelatin composite scaffolds for liver tissue engineering. *Journal of Digestive Diseases*, ***13***, 168-178.

[4] **Orlova, A. A., Kotlyarova, M. S., Lavrenov, V. S., Volkova, S. V., Arkhipova, A. Y.** 2014. Relationship between Gelatin Concentrations in Silk Fibroin-Based Composite Scaffolds and Adhesion and Proliferation of Mouse Embryo Fibroblasts. *Bulletin of Experimental Biology and Medicine*, ***158***, 88-91.

[5] **Teimouri, A., Azadi, M., Emadi, R., Lari, J., Chermahini, A. N.** (2015). Preparation, characterization, degradation and biocompatibility of different silk fibroin based composite scaffolds prepared by freeze-drying method for tissue engineering application. *Polymer Degradation and Stability*, ***121***, 18-29.

[6] **Kamolz, L. P., Koch, H., Kasper, C.** (2013).Tissue engineering and its potential use in surgery. *European Surgery*, ***45***, 120-121.

[7] **Jetbumpenkul, P., Amornsudthiwat, P., Kanokpanont, S., Damrongsakkul, S.** (2012). Balanced electrostatic blending approach – An alternative to chemical crosslinking of Thai silk fibroin/gelatin scaffold. *International Journal of Biological Macromolecules*, ***50***, 7-13.

[8] **Gould, D.** (2014). Tissue Engineering for Plastic Surgeons: A Primer Commentary. *Aesthetic Plastic Surgery*, ***38***, 222-223.

[9] **Dvir, T., Timko, B. P., Kohane, D. S., Langer, R.** (2011). Nanotechnological strategies for engineering complex tissues. *Nature Nanotechnology*, ***6***, 13-22.

[10] **Bhardwaj, N., Chakraborty, S., Kundu, S. C.** (2011). Freeze-gelled silk fibroin protein scaffolds for potential applications in soft tissue engineering. *International Journal of Biological Macromolecules*, ***49***, 260-267.

[11] **Chomchalao, P., Pongcharoen, S., Sutheerawattananonda, M., Tiyaboonchai, W.** (2013). Fibroin and fibroin blended three

dimensional scaffolds for rat chondrocyte culture. *International Journal of Biological Macromolecules*, ***12:28***, 1-12.

[12] **Tritanipakul, S., Kanokpanont, S., Kaplan, D. L., Damrongsakkul,S.** (2009). Morphology and In Vitro Biocompatibility of Hydroxyapatite-Conjugated Gelatin/Thai Silk Fibroin Scaffolds. *IFMBE Proceedings*, ***23***, 1377-1380.

[13] **Tiyaboonchai, W., Chomchalao,P., Sutheerawattananonda, M., Sobhon, P., Pongcharoen, S.** (2011). Preparation and Characterization of Blended *Bombyxmori* Silk Fibroin Scaffolds. *Fibers and Polymers*, ***3***, 324-333.

[14] **Wongputtaraksa, T., Ratanavaraporn, J., Pichyangkura, R.,Damrongsakkul, S.** (2012). Surface modification of Thai silk fibroin scaffolds with gelatin and chitooligosaccharide for enhanced osteogenic differentiation of bonemarrow-derived mesenchymal stem cells. *Journal Of Biomedical Materias Research B: Applied Biomaterials*, ***8***, 2307-2315.

[15] **Subia, B., Kundu, J., Kundu, S. C.** (2010). Biomaterial scaffold fabrication techniques for potential tissue engineering applications. *Tissue Engineering*,141-158.

[16] **Mandal, B. B. and Kundu, S. C.** (2009).Cell proliferation and migration in silk fibroin 3D scaffolds. *Biomaterials*, ***30***, 2956-2965.

[17] **Sa, M. W. and Kim, J. Y.** (2013). Design of multi-scaffold fabrication system for various 3D scaffolds. *Journal of Mechanical Science and Technology*, ***10***, 2961-2966.

[18] Smart Freeze Drying – Basic principles, optimum procedures and applications. (2010). *Martin Christ Gefriertrocknungsanlagen GmbH*.

[19] **Nireesha, G. R., Divya, L., Sowmya, C., Venkateshan, N., Babu, M. N., Lavakumar, V.** (2013). Lyophilization/Freeze Drying - An Review. *International Journal of Novel Trends in Pharmaceutical Sciences*, ***3***, 87-98.

[20] **Gualandi, C.** (2011). *Time Porous Polymeric Bioresorbable Scaffolds forTissue Engineering*. Heidelberg: Springer-Verlag.

[21] **Ikada, Y.** (2006). *Tissue Engineering: Fundamentals and Applications*. Cambridge: Academic Press.

[22] **Whang, K., Thomas, C. H., Healy, K. E.**(1995). A novel method to fabricate bioabsorbable scaffolds. *Polymer*, ***36***, 837-842.

[23] **Baheti, A., Kumar, L., Bansal, A. K.** (2010). Excipients used in lyophilization of small molecules. *Journal of Excipients and Food Chemicals*, ***1***, 41-54.

[24] **Sultana, N., Hassan, M. I., Lim, M. M.** (2015). *Composite Synthetic Scaffolds for Tissue Engineering and Regenerative Medicine*. Heidelberg: Springer-Verlag.

[25] **Chahal, S., Hussain, F. S. J., Kumar, A., Rasad, M. S. B. A., Yusoff, M. M.** (2016). Fabrication, characterization and *in vitro* biocompatibility of electrospun hydroxyethylcellulose/poly(vinyl)alcohol nanofibrous

composite biomaterial for bone tissue engineering. *Chemical Engineering Science*, ***144***, 17-29.

[26] **Zulkifli, F. H., Hussain, F. S. J., Rasad, M. S. B. A.,Yusoff, M. M.** (2014). Nanostructured materials from hydroxyethyl cellulose for skintissue. *Carbohydrate Polymers*, ***114***, 238-245.

[27] **Vaikkath, D., Anitha, R., Sumathy, B., Nair, P. D.** (2016). A simple and effective method for making multipotent/multilineage scaffolds with hydrophilic nature without anypostmodification/treatment. *Colloids and Surfaces B: Biointerfaces*, ***141***, 112-119.

[28] **Wendorff, J. H., Agarwal, S., Greiner, A.** (2012). *Electrospinning: Materials, Processing, and Applications*. Weinheim: Wiley-VCH Verlag GmbH & Co. KGaA.

[29] **Zhang, Q., Li, M., Liu, J., Long, S., Yang, J., Wang, X.** (2012). Porous ultrafine fibers via a salt-inducedelectrospinningmethod. *Colloid and Polymer Science*, ***290***, 793–799

[30] **Wray, L. S., Hu, X., Gallego, J., Georgakoudi, I., Omenetto, F. G., Schmidt, D., Kaplan, D. L.**(2011). Effect of Processing on Silk-Based Biomaterials: Reproducibility and Biocompatibility. *International Journal of Biomedical Materials Research B Applied Biomaterials*, ***99***, 89-101.

[31] **Kovacina, J. R., DesRochers, T. M., Burke, K. A., Kaplan, D. L.** (2015). The Effect of Sterilization on Silk Fibroin Biomaterial Properties. *Macromolecular Bioscience*, ***15***, 861-874.

[32] **Kundu, B., Rajkhowa, R., Kundu, S. C., Wang, X.** (2013). Silk fibroin biomaterials for tissue regenerations. *Advanced Drug Delivery Reviews*, ***65***, 457-470.

[33] **Pan, H., Zheng, Q., Guo, X., Wu, Y., Wu, B.** (2016). Polydopamine-assisted BMP-2-derived peptides immobilization on biomimetic copolymer scaffold for enhanced bone induction *in vitro* and *in vivo. Colloids and Surfaces B: Biointerfaces*, ***142***, 1-9.

[34] **Lanza, R., Langer, R., Vacanti, J.** (2014). *Principles of Tissue Engineering*. Cambridge: Academic Press.

[35] **Sheets, K. T.** (2010). *Mechanical and Cellular Response to Biomineralization of Ovalbumin Scaffolds for Bone Tissue Engineering* (Master of Science thesis). Virginia Polytechnic Institute and State University, Blacksburg.

[36] **Shachar, M., Tsur-Gang, O., Dvir, T., Leor, J., Cohan, S.** (2011). The effect of immobilized RGD peptide in alginate scaffolds on cardiac tissue engineering. *Acta Biomaterialia*, ***7***, 152-162.

[37] **Gentile, P., Nandagiri, V. K., Daly, J., Chiono, V., Mattu, C., Tonda-Turo, C., Ciardelli, G., Ramtoola, Z.** (2016). Localised controlled release of simvastatin from porous chitosan–gelatin scaffolds engrafted with simvastatin loaded PLGA-microparticles for bone tissue engineering application. *Materials Science and Engineering C*, ***59***, 249-257.

[38] **Pan, T., Song, W., Cao, X., Wang, Y.** (2016). 3D Bioplotting of Gelatin/Alginate Scaffolds for Tissue Engineering: Influence of Crosslinking Degree and Pore Architecture on Physicochemical Properties. *Journal of Materials Science & Technology*, 1-12.

[39] **Graulus, G. J., Mignon, A., Van Vlierberghe, S., Declercq, H., Feher, K., Cornelissen, M., Martinus, J. C:,Dubruel, P.** (2015). Cross-linkable alginate-graft-gelatin copolymers for tissue engineering applications. *European Polymer Journal*, ***72***, 494-506.

[40] **Ivanova, E. P., Bazaka, K., Crawford, R. J.** (2014). *New functional biomaterials for medicine and healthcare*. Sawston: Woodhead Publishing.

[41] **Klotz, B. J., Gawlitta, D., Rosenberg, A. J. W. P., Malda, J., Melchels, F. P. W.** (2016). Gelatin-Methacryloyl Hydrogels: Towards Biofabrication-Based Tissue Repair. *Trends in Biotechnology*, ***34***, 394-407.

[42] **Li, X. K., Cai, S. X., Liu, B., Xu, Z. L., Dai, X. Z., Ma, K. W., Li, S. Q., Yang, L., Sung, K. L. P., Fu, X. B.** (2007). Characteristics of PLGA–gelatin complex as potential artificial nerve scaffold. *Colloids and Surfaces B: Biointerfaces,****57***, 198-203.

[43] **Kakkar, P., Verma, S., Manjubala, I., Madhan, B.** (2014). Development of keratin–chitosan–gelatin composite scaffold for soft tissue engineering. *Materials Science and Engineering C*, ***45***, 343-347.

[44] **Kovacina, J. R., DesRochers, T. M., Burke, K. A., Kaplan, D. L.** (2015). The Effect of Sterilization on Silk Fibroin Biomaterial Properties. *Macromolecular Bioscience*, ***15***, 861-874.

[45] **Lu, Q., Zhang, X., Hu, X., Kaplan, D. L.** (2010). Green Process to Prepare Silk Fibroin/Gelatin Biomaterial Scaffolds. *Macromolecular Bioscience,****10***, 289-298.

[46] **Zhang, H., Li, L. L., Dai, F. Y., Zhang, H. H., Ni, B., Zhou, W., Yang, X., Wu, Y. Z.** (2012). Preparation and characterization of silk fibroin as a biomaterial with potential for drug delivery. *Journal of Translational Medicine*, ***10***, 1-9.

[47] **Kambe, Y., Kojima, K., Tamada, Y., Tomita, N., Kameda, T.** (2016). Silk fibroin sponges with cell growth-promoting activity induced by genetically fused basic fibroblast growth factor. *Society for Biomaterials*, ***104A***, 82-93.

[48] **Kaewprasit, K., Promboon, A., Kanokpanont, S., Damrongsakkul, S.** (2014). Physico-chemical properties and *in vitro* response of silk fibroin fromvarious domestic races. *Society for Biomaterials*, ***102B***, 1639-1647.

[49] **He, J., Liu, Y., Hao, X., Mao, M., Zhu, L., Li, D.** (2012). Bottom-up generation of 3D silk fibroin–gelatin microfluidic scaffolds with improved structural and biological properties. *Materials Letters,****78***, 102-105.

[50] **Sawatjui, N., Damrongrungruang, T., Leeanansaksiri, W., Jearanaikoon, P., Limpaiboon, T.** (2014). Fabrication and characterization of silk

fibroin–gelatin/chondroitinsulfate/hyaluronicacid scaffold for biomedical applications. *MaterialsLetters*, ***126***, 207-210.

[51] **Liu, B., Song, Y. W., Jin, L., Wang, Z. J., Pu, D. Y., Lin, S. Q., Zhou, C., You, H. J., Ma, Y., Li, J. M., Yang, L., Sung, K. L. P., Zhang, Y. G.** (2015). Silk structure and degradation. *Colloids and Surfaces B: Biointerfaces*, ***131***, 122-128.

[52] **Wray, L. S., Hu, X., Gallego, J., Georgakoudi, I., Omenetto, F. G., Schmidt, D., Kaplan, D. L.** (2011). Effect of processing on silk-based biomaterials: Reproducibility and biocompatibility. *Journal of Biomedical Materials Research B: Applied Biomaterials*, ***99B***, 89-101.

[53] **Kundu, B., Kurland, N. E., Bano, S., Patra, C., Engel, F. B., Yadavalli, V. K., Kundu, S. C.** (2014). Silk proteins for biomedical applications: Bioengineering perspectives. *Society for Biomaterials*, ***39***, 251-267.

[54] **Hardy, J. G., Scheibel, T. R.** (2010). Composite materials based on silk proteins. *Progress in Polymer Science*, ***9***, 1093-1115.

[55] **Cheng, Y., Koh, L. D., Li, D., Ji, B., Han, M. Y., Zhang, Y. W.** (2016). On the strength of β-sheet crystallites of *Bombyxmori* silk fibroin. *Journal of The Royal Society*, ***11***, 1-8.

[56] **Zhang, C., Song, D., Lu, Q., Hu, X., Kaplan, D. L., Zhu, H.** (2012). Flexibility regeneration of silk fibroin in vitro. *Biomacromolecules*, ***13***, 2148-2153.

[57] **Li, G., Liu, H., Li, T., Wang, J.** (2012). Surface modification and functionalization of silk fibroin fibers/fabric toward high performance applications. *Materials Science and Engineering C*, ***32***, 627-636.

[58] **Hu, X., Kaplan, D., Cebe, P.** (2006). Determining Beta-Sheet Crystallinity in Fibrous Proteins by Thermal Analysis and Infrared Spectroscopy. *Macromolecules*, ***39***, 6161-6170.

[59] **Dubruel, P. and Vlierberghe, S. V.** (2014). *Biomaterials for Bone Regeneration.* Amsterdam: Elsevier Ltd.

[60] **Tomlins, P.** (2015). *Characterisation and Design of Tissue Scaffolds*. Amsterdam: Elsevier Ltd.

[61] **Haaparanta, A. M., Jaervinen, E., Cengiz, İ. F., Ellae, V., Kokkonen, H. T., Kiviranta, I., Kellomaeki, M.** (2014). Preparation and characterization of collagen/PLA, chitosan/PLA, and collagen/chitosan/PLA hybrid scaffolds for cartilage tissue engineering. *Journal of Materials Science: Materials in Medicine*, ***25***, 1129–1136

[62] **Gautam, S., Chou, C. F., Dinda, A. K., Potdar, P. D., Mishra, N. C.** (2014). Fabrication and characterization of PCL/gelatin/chitosan ternary nanofibrous composite scaffold for tissue engineering applications. *Journal of Materials Science*, ***49***, 1076-1089.

[63] **Shavandi, A., Bekhit, A. E. A., Sun, Z., Ali, M. A.** (2016). Injectable gel from squid pen chitosan for bone tissue engineering applications. *Journal of Sol-Gel Science and Technology*, ***77***, 675-687.

[64] **Hu, J. X., Cai, X., Mo, S., Chen, L., Shen, X., Tong, H.** (2015). Fabrication and Characterization of Chitosan-Silk Fibroin/Hydroxyapatite Composites via *in situ* Precipitation for Bone Tissue Engineering. *Chinese Journal of Polymer Science*, ***33***, 1661-1671.

[65] **Croisier, F. and Jerome, C.** (2013). Chitosan-based biomaterials for tissue engineering. *European Polymer Journal*, ***49***, 780-792.

[66] **Oh, J., Kim, K., Won, S. W., Cha, C., Gaharwar, A. K., Selimovic, S., Bae, H., Lee, K. H., Lee, D. H., Lee, S. H., Khademhosseini, A.** (2013). Microfluidic fabrication of cell adhesive chitosan microtubes. *Biomedical Microdevices*,***15***, 465-472.

[67] **Shaik, M. M. and Kowshik, M.** (2016). Novel melt-down neutralization method for synthesis of chitosan–silver scaffolds for tissue engineering applications. *Polymer Bulletin*, ***73***, 841-858.

[68] **Fernandez-Yague, M. A., Abbah, S. A., McNamara, L., Zeugolis, D. I., Pandit, A., Biggs, M. J.** (2015). Biomimetic approaches in bone tissue engineering: Integrating biological and physicomechanical strategies. *Advanced Drug Delivery Reviews*,***84***, 1-29.

[69] **Saravanan, S., Leena, R. S., Selvamurugan, N.** (2016). Chitosan based biocomposite scaffolds for bone tissue engineering. *International Journal of Biological Macromolecules*, 1-12.

[70] **Basha, R. Y., Kumar, S., Doble, M.** (2015). Design of biocomposite materials for bone tissue regeneration. *Materials Science and Engineering: C*,***57***, 452-463.

[71] **Melke, J., Midha, S., Ghosh, S., Ito, K., Hoffmann, S.** (2015). Silk fibroin as biomaterial for bone tissue engineering. *ActaBiomaterialia*, ***31***, 1-16.

[72] **Varkey, A., Venugopal, E., Sugumaran, P., Janarthanan, G., Pillai, M. M., Rajendran, S., Bhattacharyya, A.** (2015). Impact of silk fibroin-based scaffold structures on human osteoblast MG63 cell attachment and proliferation. *International Journal of Nanomedicine*, ***10***, 43-51.

[73] **Oyane, A., Kim, H. M., Furuya, T., Kokubo, T., Miyazaki, T., Nakamura, T.** (2003). Preparation and assessment of revised simulated body fluids. *Journal of Biomedical Materials Research Part A*, ***65A***, 188-195.

[74] **Rockwood, D. N., Preda, R. C., Yücel, T., Wang, X., Lovett, M., Kaplan, D. L.** (2011). Materials Fabrication from *Bombyx mori* Silk Fibroin, *Nature Protocols*, ***6***, 1612-1631.

[75] **Lerdchai, K., Kitsongsermthon, J., Ratanavaraporn, J., Konakpanont, S., Damgrongsakkul, S.** (2016). Thai Silk Fibroin/Gelatin Sponges for the Dual Controlled Release of Curcumin and Docosahexaenoic Acid for Anticancer Treatment, *Journal of Pharmaceutical Sciences*, ***105***, 221-230.

[76] **Kundu, S.** (2014). *Silk Biomaterials for Tissue Engineering and Regenerative Medicine*. Cambridge: Woodhead Publishing Limited.

[77] **Prasong, S., Wilaiwan, S., Nualchai, K.** (2010). Structure and Thermal Characteristics of *Bombyx mori* Silk Fibroin Films: Effect of Different

Organic Solvents. *International Journal of Chemical Technology*, ***2***, 21-27.

[78] **Baimark, Y. and Srihanam, P.** (2009). Effect of Methanol Treatment on Regenerated Silk Fibroin Microparticles Prepared by the Emulsification-Diffusion Technique. *Journal of Applied Sciences*, ***9***, 3876-3881.

[79] **Shang, S., Zhu, L., Fan, J.** (2011). Physical properties of silk fibroin/cellulose blend films regenerated from the hydrophilic ionic liquid. *Carbohydrate Polymers*, ***86***, 462-468.

[80] **Berzina-Cimdina, L. and Borodajenko, N.** (2012). *Research of Calcium Phosphates Using Fourier Transform Infrared Spectroscopy*. Rijeka: INTECH Open Access Publisher.

[81] **Cholas, R., Padmanabhan, S. K., Gervaso, F., Udayan, G., Monaco, G., Sannino, A., Licciulli, A.** (2016). Scaffolds for bone regeneration made of hydroxyapatite microspheres in a collagen matrix. *Materials Science and Engineering C*, ***63***, 499-505.

[82] **Tsiourvas, D., Sapalidis, A., Papadopoulos, T.** (2016). Hydroxyapatite/ chitosan-based porous three-dimensional scaffolds with complex geometries. *Materials Today Communications*, ***7***, 59-66.

[83] **Sharma, C., Dinda, A. K., Potdar, P. D., Chou, C., Mishra, N. C.** (2016). Fabrication and characterization of novel nano-biocomposite scaffold of chitosan–gelatin–alginate–hydroxyapatite for bone tissue engineering. *Materials Science and Engineering C*, ***64***, 416-427.

APPENDICES

APPENDIX A: Chemicals and Materials

APPENDIX B: Preparation of 1X Phosphate Buffered Saline (PBS) Buffer

APPENDIX C: Preparation of 1X Modified Simulated Body Fluid (mSBF)

APPENDIX D: Laboratory Equipment

APPENDIX A

Chemical/Material	Supplier
Methanol, CH_3OH	Sigma-Aldrich
Gelatin from bovine skin, Type B	Sigma-Aldrich
Glutaraldehyde	Sigma-Aldrich
Sodium azide, NaN_3	Merck Millipore
Silkworm cocoons	Kozabirlik
Sodium chloride, NaCl	Merck Millipore
Potassium chloride, KCl	Sigma-Aldrich
Sodium phosphate dibasic, Na_2HPO_4	Sigma-Aldrich
Potassium phosphate monobasic, KH_2PO_4	Sigma-Aldrich
Lithium bromide, LiBr	Sigma-Aldrich
Di-potassium hydrogen phosphate, HK_2O_4P	Sigma-Aldrich
4-(2-hydroxyethyl)-1-piperazineethanesulfonic acid	Biomatik
Magnesium chloride, Cl_2Mg	Sigma-Aldrich
Sodium sulphate, Na_2SO_4	Sigma-Aldrich
Sodium bicarbonate, $CHNaO_3$	Sigma-Aldrich
Calcium chloride, $CaCl_2$	Sigma-Aldrich
Sodium carbonate, Na_2CO_3	Sigma-Aldrich
Hydrochloride, HCl	Sigma-Aldrich
Sodium hydroxide, NaOH	Sigma-Aldrich
Protease XIV	Sigma-Aldrich

APPENDIX B

1. The following materials were weighed in the amount mentioned below and dissolved in 800 mL ultrapure water:
    - 8 g of sodium chloride (NaCl)
    - 0.2 g of potassium chloride (KCl)
    - 1.44 g of sodium phosphate dibasic (Na_2HPO_4)
    - 0.24 g of potassium phosphate monobasic (KH_2PO_4)
2. The pH of the solution was adjusted to 7.4 with hydrochloride (HCl).
3. The total volume of the solution was adjusted to 1 litre with ultrapure water.
4. The solution was sterilised by filtration.

APPENDIX C

1. All apparatus to be used for preparation of mSBF solution were washed with 1.0 M of HCl and ultrapure water.
2. 700 mL of ultrapure water were poured into a 1 litre polypropylene beaker that was stirred using a magnetic bar at room temperature.
3. The reagents listed below were added according to the order and amounts given in the list and completely dissolved. The HEPES was previously dissolved in 100 mL of aqueous 0.2 M NaOH.
    1. NaCl: 5.403 g
    2. $NaHCO_3$: 0.504 g
    3. Na_2CO_3: 0.426 g
    4. KCl: 0.225 g
    5. $K_2HPO_4.3H_2O$: 0.230 g
    6. $MgCl_2.6H_2O$: 0.311 g
    7. HEPES: 17.892 g
    8. $CaCl_2$: 0.293 g
    9. Na_2SO_4: 0.072 g
    10. NaOH (1.0 M): 15 mL
4. The fluid was adjusted to a final pH of 7.4 at room temperature by titrating aqueous 1.0 M of HCl into the fluid.
5. The total volume of the fluid was adjusted to 1 litre by adding ultrapure water.
6. The freshly prepared mSBF solution was sterilised by using 0.22 pore size filters.
7. The solution was stored at 4 ^{o}C until biomineralisation assays.

In order to prepare a 3X mSBF solution, the amounts of the ingredients above were multiplied by 3. All remaining steps were applied in the same way.

APPENDIX D

Equipment	**Supplier**
Refrigerator, +4 ^{o}C	Vestel
Magnetic stirrer	Cole-Parmer
Scale	Precisa Gravimetrics AG
Freezer, -20 ^{o}C	Arçelik
Freeze-dryer	Martin Christ
pH metre	WTW GmbH
Rocking platform shaker	Heidolph Instruments
Heating/Drying oven	Memmert GmbH + Co. KG
Centrifuge	Beckman Coulter
Pipettes	Eppendorf
Beakers	ISOLAB
Tissue culture test plates	TPP Techno Plastic Products AG
Scanning electron microscope, SEM	FEI
Dialysis cassettes	Thermo Scientific
Syringe and needle	BD Medical
Ultrapure water system	TKA-Pacific
Fourier transform infrared spectroscopy, FTIR	Perkin Elmer

CURRICULUM VITAE

Name Surname **:** Burak AĞBABA

Place and Date of Birth **:** Sivas, 26 April 1991

E-Mail **:** agbababurak@hotmail.com

EDUCATION **:**

- **B.Sc.** **:** 2014, Yıldız Technical University, Faculty of Chemical and Metallurgical Engineering, Department of Bioengineering

PROFESSIONAL EXPERIENCE:

- Part-time Working Student, Roche Müstahzarları San. A.Ş. (March 2016 – Present)
- Part-time Intern, Pfizer İlaçları Ltd. Şti. (February 2015 – February 2016)
- Part-time Intern, Eczacıbaşı-Baxter HastaneÜrünleri San. ve Tic. A.Ş. (August 2013 – December 2014)
- Intern, Eczacıbaşı-Baxter Hastane Ürünleri San.ve Tic. A.Ş. (June 2013 – July 2013)
- Intern, Istanbul University (August 2011)